



SCHOOL of
GRADUATE STUDIES
EAST TENNESSEE STATE UNIVERSITY

East Tennessee State University
Digital Commons @ East Tennessee
State University

Electronic Theses and Dissertations

Student Works

5-2019

Telomeric DNA Damage and Repair Machineries in HIV Infection

Lam Nguyen

East Tennessee State University

Follow this and additional works at: <https://dc.etsu.edu/etd>

 Part of the [Immunology of Infectious Disease Commons](#)

Recommended Citation

Nguyen, Lam, "Telomeric DNA Damage and Repair Machineries in HIV Infection" (2019). *Electronic Theses and Dissertations*. Paper 3536. <https://dc.etsu.edu/etd/3536>

This Thesis - unrestricted is brought to you for free and open access by the Student Works at Digital Commons @ East Tennessee State University. It has been accepted for inclusion in Electronic Theses and Dissertations by an authorized administrator of Digital Commons @ East Tennessee State University. For more information, please contact digilib@etsu.edu.

Telomeric DNA Damage and Repair Machineries in HIV Infection

A thesis

presented to

the faculty of the Department of Internal Medicine and Biological Sciences

East Tennessee State University

In partial fulfillment

of the requirement for the graduate degree

Master of Science in Biology

by

Lam Ngoc Thao Nguyen

May 2019

Dr. Zhi Q. Yao, Chair

Dr. Shunbin Ning

Dr. Ling Wang

Keywords: ATM, Apoptosis, DNA damage repair, shelterin, HIV, T cell homeostasis

ABSTRACT

Telomeric DNA Damage and Repair Machineries in HIV Infection

by

Lam Ngoc Thao Nguyen

In this thesis, we investigated T cell homeostasis and DNA damage repair machineries in HIV infection. We found that the frequencies of CD4T cells were low, which is associated with cell apoptosis in HIV patients compared to healthy subjects. Importantly, these events were closely correlated to the increase in T cell exhaustion, senescence, DNA damage, and telomere attrition. Mechanistically, while the DNA damage sensors Mer11, Rad50, and NBS1 (MRN) complexes remained intact, the ataxia-telangiectasia mutated (ATM) kinase and its downstream checkpoint kinase 2 (CHK2) were significantly inhibited during HIV infection. Additionally, telomeric repeat-binding factor 2 (TRF2) that functions to protect telomeres from unwanted DNA damage was also suppressed by HIV infection. These findings revealed an important mechanism by which telomeres undergo DNA damage that remained unrepaired due to ATM deficiency and TRF2 deprotection - a process that could promote T cell apoptosis, senescence, and cellular dysfunction in HIV infection.

ACKNOWLEDGEMENTS

I would first like to thank my research advisor, Dr. Zhi Q. Yao, Director of Center of Excellence for HIV/AIDS, James H. Quillen College of Medicine, East Tennessee State University, for his dedicated guidance and advice. His door is always open whenever I need help in my research experiments and scientific writing.

I would also like to thank my academic advisor, Dr. Thomas C. Jones, the graduate coordinator of Biological Sciences, East Tennessee State University, for his instructions about courses throughout my Master of Science program. I would like to express my gratitude to my committee members, Dr. Shunbin Ning and Dr. Ling Wang for their guidance and always being supportive towards my performances.

I would also like to acknowledge Dr. Jonathan Moorman, the staff and students working in Dr. Yao's laboratory, including laboratory manager, Xiao Y. Wu; laboratory technician Zheng D. Morrison, Dr. Qiyuan Tang, Dr. Yingjie Ji, Lam Nhat Nguyen, Juan Zhao, Sushant Khanal, Xindi Dang, Dechao Cao, Stella Ogbu, Oluwayomi Oyedeji, Madison Schank for all their help and support.

Lastly, I am very grateful for all the love and support from my parents, my brother, and my fiancé. This accomplishment would not be possible without them.

This work is supported by National Institutes of Health (NIH) grants: R01DK093526, R01AI114748, R21AI138598, and R15AG050456, and by VA Merit Review Awards: 1I01BX002670, 1I01BX004281, and by a DoD Award: PR170067

TABLE OF CONTENTS

	Page
ABSTRACT.....	2
ACKNOWLEDGEMENTS.....	3
TABLE OF CONTENTS.....	4
LIST OF TABLES.....	7
LIST OF FIGURES.....	8
Chapter	
1. INTRODUCTION.....	10
2. MATERIALS AND METHODS.....	19
Ethic Statement.....	19
Subjects.....	19
Cells Isolation and Culture.....	19
Peripheral Blood Mononuclear Cells (PBMCs) Isolation.....	19
CD4 T Lymphocytes Isolation.....	21
Cell Culture.....	22
Flow Cytometry.....	22
Phenotype Analysis.....	23
Cell Apoptosis Qualification.....	24
Analysis of Interest Proteins.....	26

FCM Detailed Protocol	27
Extracellular staining	27
Intracellular staining	27
Annexin V/7-AAD staining assay	27
ROS detection	28
Flow-FISH	28
Confocal Microscopy	29
RNA Isolation and Real-time RT-PCR.....	31
Western Blotting	35
Statistical Analysis.....	37
Experimental Design.....	37
3. RESULTS	40
CD4T cell homeostasis and apoptotic susceptibility in latently HIV-infected individuals on ATR treatment	40
CD4T cell exhaustion and senescence in latent HIV infection.....	44
Telomere attrition and telomeric DNA damage in CD4T cell in latent HIV infection	46
ATM expression and activity are inhibited in CD4T cells during latent HIV infection	53

TRF2 expression and activity are inhibited in CD4T cells during latent HIV infection	58
4. DISCUSSION	61
REFERENCES	63
VITA.....	68

LIST OF TABLES

Table	Page
1. List of PCR Master Mix Components and Concentrations	32
2. cDNA Synthesis (RT) Thermo Cyclers Conditions	33
3. Real-time RT-PCR Thermo Cyclers Conditions	34
4. List of Primers used in the Study	34
5. Western Blotting Resolving Gel Preparation Components	36
6. Western Blotting Stacking Gel Preparation Components	36

LIST OF FIGURES

Figure	Page
1. Experimental design.....	38
2. Percentage of lymphocytes in PBMCs analyzed by FCM.....	41
3. Percentage of Av ⁺ /7-AAD positive CD4 populations	42
4. Pearson Correlation analysis between percentage of CD4T cells and apoptosis.....	43
5. Pearson Correlation analysis between percentage of CD4T cells and the actual CD4T cell counts in HIV-infected patients	44
6. Percentage of PD1 expression in lymphocytes and CD4T cells by FCM analysis	45
7. The percentage of CD28 and CD57 protein expressions in CD4T cells analyzed by FCM.....	46
8. Telomere length determination by Flow-FISH analysis.....	47
9. Pearson correlation analysis of the telomere length (MFI) and the percentage of early apoptotic cells.	48
10. Median Fluorescence Intensity of DCFDA in HIV patients and healthy subjects	49
11. Mean Fluorescence Intensity of CellROX Green and Annexin V in CD4T cells from HIV- infected and healthy subjects	50
12. Confocal microscope analysis of the co-localization of 53BP1 and TRF1 proteins in CD4T cells isolated from HIV-infected and healthy subjects.	51
13. Percentage and Median Fluorescence Intensity of γ H2AX determined by FCM analysis.....	52
14. Gene and protein expressions of MRN complex determined by Real-time RT-PCR and Western Blotting, respectively.....	54
15. ATM and phosphorylated ATM gene and protein expressions determined by Real-time RT- PCR and Western Blotting.....	55
16. Median Fluorescence Intensity of phosphorylated ATM measured by FCM analysis.....	56

17. Gene expression and Median Fluorescence Intensity of ATM downstream proteins determined by Real-time RT-CR.....	57
18. Protein expressions of ATM downstream molecules determined by Western Blotting.	58
19. Transcription expressions of proteins in shelterin complex determined by Real-time RT-PCR.....	59
20. Translation expressions of proteins in shelterin complex determined by Western blotting. ..	60

CHAPTER 1

INTRODUCTION

Human immunodeficiency virus (HIV) infection is known to originate from the rural areas of Central Africa in the late 1800s. It is believed that simian immunodeficiency virus (SIV), an immunodeficiency virus in chimpanzees, was transmitted from apes to humans and mutated into HIV when hunters had contact with the infected blood while handling the bush meat of the infected animals in the southeastern part of Cameroon. From there, HIV infection was present in low levels in remote Africa until it was carried down the Congo River to Leopoldville (became Kinshasa in 1986), which was a very popular growing area at the time. Over the decades, HIV infection slowly spread into other parts of Africa, and eventually became an epidemic over the world. HIV infection was first detected in the United States (US) in the mid to late 1970s ¹.

According to a report by the Centers for Disease Control and Prevention (CDC), by the end of 2015, it was estimated that approximately 1.1 million people in the US were living with HIV infection, in which about 15%, or, only 1 in 7 of that population, were aware that they were infected by HIV. There were 38,739 newly diagnosed HIV cases in the US in 2017. The most popular mode of transmission is through male to male sexual contact, followed by heterosexual contact, and intravenous drug use being the least. Studies showed that Black/African Americans were the highest population infected with HIV; this is followed by Caucasians, and Hispanics and Asians being the least affected populations. In 2016, there were 15,807 deaths in relation to HIV and acquired immunodeficiency syndrome (AIDS) in the US. HIV infection continues to cause serious global health burden with an estimated 1.8 million newly diagnosed cases in 2017; 940,000 deaths from HIV/AIDS-related health issues in 2017 and about 36.9 million people

living with HIV infection globally. Among these, only 21.7 million people have access to antiretroviral therapy (ART).

Currently, there is no effective cure for HIV/AIDS. However, HIV infection can be controlled if the infected individuals are treated with highly active antiretroviral therapy (HAART), which can effectively suppress the replication of HIV. Therefore, under effective ART, the viral load (measured by real-time RT-PCR for the amount of HIV-RNA present in blood) of infected subjects is not detectable, and this helps them to live healthy lives with little or no risk of transmitting HIV to others sexually. However, if infected individuals fail to take their ART, they would suffer serious complications from the HIV infection.

There are three stages of HIV infection. The first stage (called acute HIV infection) presents with flu-like symptoms and usually lasts for about two to four weeks. During this stage, the viral load is extremely high in the patient's blood. Following the acute phase is the clinical latency stage, also called chronic infection. During this phase, the viruses are still in the active state; however, viral replication occurs at very low levels. This phase is also associated with a decrease in the number of CD4T cells at the rate of ~100 CD4T cells/per year. This phase can last for 8-10 years and can progress to AIDS in untreated individuals. The last stage, called AIDS, is defined by CD4T cells count below 200 cells per milliliter of blood. At this stage, the patients present with chills, fever, weakness, weight loss, and AIDS defining illness. At this phase, their immune system is badly damaged and this results in opportunistic infections, malignancies, and death.

HIV is a retrovirus, which belongs to *Retroviridae* viral family. The retrovirus genome possesses a single, positive stranded RNA. As a retrovirus, it has the ability to reverse-transcribe its RNA into DNA using the reverse transcriptase enzyme. Following reverse transcription, the

viral DNA is incorporated into the host genome by an integrase. Then, the inserted viral DNA is continuously transcribed and translated together with the host DNA to produce new viruses indefinitely. HIV belongs to the *Lentivirus* subgroup which is characterized by a long incubation period, causing latent and/or chronic infection in humans and other mammalian species ².

HIV mainly targets the CD4T lymphocytes. The human immune system is divided into two main immunity mechanisms. Innate immunity is the first line of defense, which provides fast, non-specific responses to external stimulation or pathogenic infections. The other strategy is adaptive immunity. It is present only in vertebrates and provides highly specialized immune cells to fight the infectious pathogens. The cells involved in adaptive immunity are called lymphocytes. There are three main groups of lymphocytes: T cells, which mediate cellular immunity, B cells, which mediate humoral immunity, and the natural killer cells. There are two types of T lymphocytes, CD4 (T helper cells) and CD8⁺ (cytotoxic T cells) ³⁻⁴.

The interactions of HIV viral glycoproteins 120 (gp120) and the CD4receptors along with chemokine co-receptors (CCR5, CXCR4) present on the surface of T helper cells facilitate the attachment and entry of HIV, and allow for the fusion of viral particles into the host cells. Once inside the cytoplasm of host cell, viral RNA is reverse transcribed into DNA, which is then incorporated into the host genome. When activated, the host cells start to initiate transcription and translation processes to produce proteins. These proteins, together with viral polypeptides (which later fold into proteins), assemble into new viral particles, release and lead to reinfection of adjacent cells ⁵⁻⁶. The indefinite production and infection of new viral particles triggers the continuous maturation and responses of CD4T cells, which in turn trigger the responses from CD4naïve and central memory T cells to produce more effector cells in order to keep pace with the viral production rate. Long-term viral infection results in increased CD4T cells turnover,

which leads to alteration of immune homeostasis and cell loss. This is the main cause of short-lived and/or dysfunctional CD4T cells ⁷.

It has been reported that ongoing inflammation associated with progressive HIV infection is the reason for CD4T cells exhaustion, senescence, and telomere shortening. Chronic HIV infection can significantly induce DNA damage response (DDR) and cell apoptosis. While Vicente Planelles and his group reported that infectious viruses, including HIV, encode gene products that can activate the G2 cell cycle arrest, trigger the DDR, and lead to cell apoptosis ⁸; reports published by Guido Kroemer's group showed that the viral envelope glycoprotein complex activates the DDR pathway via the phosphorylation of ataxia-telangiectasia mutated (ATM) kinase and its downstream effector proteins, such as CHK2 and P53, which will eventually cause cell apoptosis ⁹. Also, Dorota Piekna-Przybylska's group suggested that *in vitro* HIV-infected cell lines induce deficiency of the DDR even though the viruses are in the latent phase ¹⁰. Taken together, these reports suggest that chronic HIV infection induces DNA damage in exhausted and senescent CD4T cells. Despite intensive research, the mechanisms by which HIV infection causes DNA damage, cellular apoptosis, and senescence remain poorly understood.

There are several proposed mechanisms by which HIV infection causes DNA damage and telomere erosion. One possibility may be the insufficiency in the DNA repair kinase ATM, along with its downstream signaling kinase CHK2 in HIV-infected CD4T cells. ATM, ATR and Rad3-Related (ATR), and DNA-dependent protein kinase c (DNA-PKc) are the main DNA repair enzymes, and they belong to the phosphatidylinositol-3-kinase-like kinase family (PIKKs). While the ATR pathway responds to single-stranded DNA breaks (SSBs), ATM and DNA-PKc facilitate the repair of double-stranded DNA breaks (DSBs) ¹¹. Following DSBs, the MRN

complex, which is formed by the association of MRE11, RAD50 and Nijmegen breakage syndrome (NBS1), acts as the sensor of the ATM pathway, quickly moving to the site of DNA break and recruiting ATM. ATM is the main transducer of this pathway. Binding of ATM to both the DNA sequence and the MRN complex triggers auto-phosphorylation and activation of ATM which in turn, phosphorylates mediator proteins, such as tumor suppressor p53-binding protein 1 (53BP1), mediator of DNA damage checkpoint protein 1 (MDC1) and checkpoint kinase 2 (CHK2). These phosphorylated mediator proteins activate tumor protein 53 (p53) which is the main effector protein of the ATM pathway. When active, effector protein p53 transduces cell signaling and induces the DNA damage repair machineries in order to protect genomic integrity.

There are four main events involved in DDR. These include cell cycle arrest, DNA repair, cellular apoptosis, and chromatin remodeling. Despite occurring independently, ATM plays a central role in all of the processes. In the first event, DSBs trigger auto-phosphorylation of ATM and phosphorylation of γ H2AX. This sets up the signaling cascade and is closely followed by the phosphorylation of CHK2. Phosphorylation of CHK2 activates p53 (acts as transcription factor) and moves to the nucleus where it initiates the transcription of p21 protein. Activated p21 protein leads to the inhibition of cyclin-dependent kinases, such as CDK2, CDK4, and CDK6 whose functions are to block the entry of cells from G1 to S phase. This cell cycle arrest is crucial as it prevents the replication of damaged DNA.

Furthermore, ATM and CHK2 proteins phosphorylate Wee1 and CDC25 proteins; thus, inhibit the activation of CDK1 protein, whose main function is to facilitate the entry into the G2/M cell cycle. Once the cell cycles are stalled, damaged DNA is repaired by efforts of non-homologous ends joining (NHEJ) or homologous recombination (HR) mechanisms. However, if

the DNA damage is irreparable, p53 protein is phosphorylated by ATM, activating several pro-apoptotic factors, such as PUMA, Bax, Bak and Nox. These factors enhance the permeability of mitochondrial membrane, leading to the leakage of cytochrome C as well as other luminal contents which activate apoptosis¹²⁻¹⁵. In general, there are many proteins that participate in the ATM DDR; however, the crucial proteins are the MRN complex, ATM, CHK2 and p53 proteins. Dysfunction or deficiency of any of these proteins results in the impairment of this important pathway, causing an increase in the level of un-repaired DNA damage. Thus, affecting genomic integrity and cell survival.

ATM deficiency has been implicated in a wide range of cellular and systemic diseases. Studies done in both cell lines and mice models revealed that ATM deficiency led to genome instability as evidenced by nuclear accumulation of 53BP1 and γ H2AX, chromosomal abnormalities, and inactivation of Poly (ADP-ribose) polymerase (PARP) protein which functions as a base excision repair protein. In addition, it has been linked to persistent DNA damage, chromosomal alterations, and increased sensitivity to radiation. These aberrant events have been shown to have close association with cancers such pancreatic and prostate cancer in mice models¹⁶, as well as B cell lymphoma, leukemia¹⁷, and human rheumatoid arthritis¹⁸. The mechanism by which ATM depletion results in malignancy is poorly understood. However, a report attributed this to oncogenic activation of WD repeat and SOCS box-containing protein 1 (WSB1): an E3-ubiquitin ligase, which in turn negatively regulates the expression of ATM by promoting ATM ubiquitination at K1323 and K2025 positions¹⁹. Anthony T Tubbs and Barry P Sleckmanin, in their study with mice models, revealed that a mutation in the ATM gene led to a defect in T cell maturation; and therefore, defects in cell cycle checkpoint dysfunction, hypersensitivity to γ irradiation, and increase in lymphoma incidence²⁰. Similarly, a study with

human models revealed that individuals with the aggressive type of T prolymphocytic leukemia (T-PLL) had a deletion in the long arm of chromosomal 11 (where the ATM gene is encoded). Furthermore, the deletion of 11q22-23 in the chromosome resulted in the accumulation of mature CD5⁺ B cells, causing B cell chronic lymphocytic leukemia: the most common type of hematologic malignancy due to ATM deficiency²¹. While ATM deficiency and its role in malignancy have been extensively studied *in vitro* and in animal models, there have been very few reports about the role of ATM dysfunction in HIV infections.

Dysfunction of the telomeres and its associated binding proteins could be another contributing factor to the increase in DNA damage and cellular apoptosis in latent HIV infection. Telomeres are repetitive nucleotide sequences, bound by several telomeric interacting proteins which function to protect the chromosomal ends from degradation and DNA damage. Telomeric DNA consist of double-stranded hexameric tandem repeats (TTAGGG) and single-stranded 3' G-rich overhangs. Telomeres are continuously lengthened by telomerase, a unique ribonucleoprotein complex consisting of a catalytic subunit, telomerase reverse transcriptase enzyme (TERT), and a telomere RNA complex component (TERC) that acts as a template for telomere extension. The telomere is in turn protected by a complex of six proteins, known as shelterin or telosome. Those proteins are telomeric repeat-binding protein 1 (TRF1), telomeric repeat-binding protein 2 (TRF2), TRF1 and TRF2 interacting nuclear protein 2 (TIN2), protection of telomere 1 (POT1), TIN2 and POT1 interacting protein 1 (TPP1), and repressor activator protein 1 (RAP1). The assembly of the shelterin complex on telomeric DNA begins with the binding of TRF1 and TRF2 proteins to the double-stranded repeat DNA sequence, which then recruits the presence of TIN2 and RAP1 proteins. TIN2 protein in turn recruits the TPP1 and POT1 complex to the nucleus²²⁻²⁴. While the telomeres play a crucial role in

preventing cellular senescence and maintaining genome integrity, telomeric attrition or dysfunction triggers the DDR machinery causing cell apoptosis.

In a study using mice models, components of the shelterin complex were knocked out *in vitro* by CRISPR/Cas9. The results showed that TRF2 and RAP1 knockout (KO) had little impact on the binding of TRF1 to the double-stranded DNA. In contrast, knock out of TIN2 significantly affected the functions of both TPP1 and POT1 proteins. Similarly, the KO of POT1 or TPP1 had great impacts on TIN2 function. Taken together, it was suggested that these three proteins formed a tight complex that was critical for telomere assembly. Furthermore, the study also showed that the KO of proteins induced a great amount of telomere dysfunction-induced foci (TIF), which recruit and increase the activity of the DDR proteins. For example, KO of TRF2 activated the ATM pathway while POT1 or TPP1 KO recruited the ATR pathway²⁵. In another study, it was indicated that telomeric DNA damage was irreparable and caused persistent TIF²⁶.

In another study, irradiated cells were examined by confocal microscopy for DDR foci. Microscopic analysis revealed that the telomeres were more prone to oxidative DNA damage and that these damages were poorly repaired in comparison to those occurring at other parts of the chromosome. This was attributed to the greater length of repeated G sequences of telomeres²⁷. Telomere dysfunction has been linked to blood disorders in humans. For example, dyskeratosis congenita (DC), an inherited disorder characterized by an abnormal skin pigmentation and nail dystrophy is thought to occur as a result of telomere dysfunction²⁸. Similarly, Werner Syndrome (WS), a very rare premature aging disease has been thought to be due to telomere attrition. These individuals have shortened telomeres, altered telomerase activity, and mutations in helicase, which is required for extension of G-rich telomeres²⁹.

The role of ATM kinase and the telomere proteins in protecting genome integrity was explored in individuals infected with Hepatitis C Virus (HCV). Zhao *et al* reported that chronic HCV infection inhibited ATM expression and activation, resulting in naïve CD4T cell DNA damage and apoptosis³⁰. Similarly, TRF2 inhibition accelerated telomere erosion and DNA damage in individuals with chronic HCV infection³¹. The above studies have emphasized the importance of the telomere and shelterin complex, as well as ATM and DDR proteins in maintaining genomic integrity and stability. Thus, impaired function of any of these factors would have an enormous negative impact on the cell signaling pathway.

The hypothesis for this research is that latent HIV infection alters the function of ATM and the shelterin proteins and may lead to DNA damage and cellular apoptosis.

CHAPTER 2

MATERIALS AND METHODS

Ethics Statement

The study protocol was approved by the institutional review board (IRB) of East Tennessee State University (ETSU) and James H. Quillen VA Medical Center (ETSU/VA IRB, Johnson City, Tennessee State). All individuals that participated in the projects were adults and signed informed consent forms.

Subjects

Two populations participated in this study, including 150 latently HIV infected patients and 166 age-matched healthy subjects (HS). HIV-infected individuals were on ART treatment, therefore they were virologically suppressed for HIV replication, as evidenced with undetectable HIV-RNA level in their blood samples. HS were supplied by Physicians Plasma Alliance (PPA, Gray, TN), and they were detected to be negative for HIV, hepatitis B virus (HBV), and hepatitis C virus (HCV) infections.

Cells Isolation and Culture

Peripheral Blood Mononuclear Cells (PBMCs) Isolation

PBMCs are peripheral blood mononuclear cells. Human PBMCs consist of the following cell populations: T lymphocytes, B lymphocytes, natural killer cells (NKs), monocytes and dendritic cells. The frequencies of these populations are different among individuals; however, typically the lymphocytes (including T lymphocytes, B lymphocytes, and NKs) account for around 70 to 90 percent, monocytes occupy 10 to 15 percent, and the dendritic cell population is

only 1 to 2 percent. In the lymphocyte population, T lymphocytes accounted for 70 percent with a ratio of 2:1 for CD4T cells and CD8⁺ T cells, respectively. B lymphocytes accounted for 5 to 10 percent and NKs occupies 5 to 15 percent³². Since CD4T cells are the main interest cells in this study, they are isolated from the mixture of cell populations in the PBMCs. The main reagent used in PBMCs isolation is Ficoll–Paque solution (GE Healthcare, Piscataway, NJ) and is applied in the technique called density gradient centrifugation separation of mononuclear cells.

In brief, the anticoagulant-treated whole blood is diluted with RPMI 1640 medium with the ratio of 1:1, and then carefully placed on top of the Ficoll-Paque solution without intermixing in the centrifugation tube. Then the tube is taken for centrifugation, which will give rise to the formation of layers containing different cell types due to differential migration of cells during the centrifugation. The bottom layer is the erythrocytes, which was aggregated by the Ficoll-Paque solution, therefore these cells penetrated through the solution to reach the bottom of the tube. The immediate layer above the erythrocytes contains the granulocytes. The next layer is the Ficoll-Paque solution, while the top layer is the plasma. The interface layer between the Ficoll-Paque solution and the plasma contains the mononuclear cells.

The anticoagulant-treated whole blood was placed into 50 ml centrifugation tube and centrifuged at 1500 rpm with acceleration and de-acceleration speeds at 9 for 5 minutes at room temperature. The result was the formation of the two layers, in which the top layer contained the plasma and the bottom layers contained the mixture of cell populations. The top layer containing plasma was removed by pipette, and the remaining solution was mixed thoroughly with the RPMI 1640 media with a ratio of 1:1. The mixture was then placed carefully on top of the Ficoll-Paque solution in another 50 ml centrifugation tube without intermixing. Then the tube was centrifuged at 2000 rpm with acceleration and de-acceleration speeds at 1 for 20 minutes at room

temperature. After the centrifugation, the solution in the tube was separated into layers from the bottom to the top with following orders: erythrocytes, granulocytes, Ficoll-Paque solution, mononuclear cells and remaining plasma and platelets. The mononuclear cells were collected and transferred into another sterile 50 ml centrifugation tube, then mixed with RPMI 1640 media. After that, the tube was centrifuged at 1800 rpm with acceleration and de-acceleration speeds at 9 for 8 minutes to produce the two layers solution. The bottom layer contained the mononuclear cells and the upper layer contained RPMI 1640 media and remaining platelets. The upper layer was then removed and the remaining mononuclear cells could be freshly used for cell isolation or could be frozen for later use. If the cells were frozen, they were mixed with RPMI 1640 media containing DMSO. The mixture was then transferred into cryotubes so that each of the tube contained 1 ml of media and 1×10^7 cells. These tubes were stored in liquid nitrogen for later use.

CD4 T Lymphocytes Isolation

CD4T cells were isolated from PBMCs using the CD4T cell negative selection kit purchased from Miltenyi Biotec Inn., Auburn, CA.

PBMCs are incubated with cocktails of biotin-conjugated monoclonal anti-human antibodies against CD8, CD14 CD15, CD16, CD19, CD36, CD56, CD123, TCR γ/δ and CD235a cells, except for CD4 cells, which are the non-target cells. Then the mixture of PBMCs and antibodies are incubated with Microbeads which are both conjugated to the monoclonal anti-biotin antibodies and magnetically tagged. The mixture is transferred and allowed to flow through the magnetic column in which the magnetically labeled cells are captured inside the column, while the unlabeled cells flow through.

PBMCs were washed with RPMI 1640 media by mixing together in a 5 ml centrifugation tube, then centrifuged at 1200 rpm for 5 minutes at room temperature. The supernatant was then removed. The cell pellet was re-suspended in 40 μ l isolation buffer and 10 μ l of antibody cocktail per 10⁷ total cells. Then the mixture was incubated at 4 – 8°C for 5 minutes. After incubation, 30 μ l of isolation buffer and 20 μ l of microbeads were added into the tube and incubated at 4 – 8°C for another 10 minutes. The magnetic column was prepared by being washed with 3 ml of isolation buffer. The incubated mixture was transferred into the column and the flow through solution was collected and placed into a new 5 ml centrifugation tube, and centrifuged at 1200 rpm for 5 minutes. The supernatant was removed, the cell pellet was re-suspended with RPMI 1640 media, called complete media, which had 10% fetal bovine serum (FBS) (Atlanta Biologicals, Flowery Branch, GA), 100 IU/ml penicillin and 2mM L-glutamine (Thermo Scientific, Logan, Utah) added. Followed by that, the re-suspended cells were taken for cell density determination.

Cell Culture

The isolated CD4 T cells were seeded into cell culture plates and incubated in an incubator at 37°C and 5% CO₂ atmosphere. After 4 days, cultured CD4 cells were harvested and used for the necessary assays.

Flow Cytometry

Flow cytometry (FCM) is a useful and rapid tool that is used extensively in scientific research for cellular characteristic classification in which the information obtained provides both quantitative and qualitative data. FCM classifies cells into distinct populations by measuring their individual optical and fluorescence characteristics. Cell components, such as DNA or RNA

can be fluorescently tagged and analyzed by FCM. In addition, antibodies conjugated with fluorescent dyes can be used to tag specific proteins, including plasma membrane, nuclear membrane, and cytosolic proteins which present in different cell types. After being fluorescently labelled, the cells are allowed to run through the flow cytometer, by which they pass its light source and become excited to a higher energy and give rise to the high energy emission. These emissions, or light signals, are immediately detected by photomultiplier tubes and digitized for computer analysis. All modern flow cytometers provide multiple fluorescent channels which allows for the analysis of several cell properties simultaneously. In this project, FCM was used to study different characteristics of distinct cellular populations since each cell type examined express different specific proteins, also referred as markers. In addition, cells belonging to one cell type also express disparate markers at certain states ³³.

Phenotypic Analysis

In order to be separated from the mixture of cellular populations in PBMCs, interested cell types were bound with specific fluorescent conjugated antibodies and were classified by FCM. In this project, CD4 cells were the main target to be studied, therefore, total CD4 and its subpopulations were sorted and their characteristics were analyzed by FCM. The extracellular marker of total CD4 was CD4⁺, naïve CD4 was CD4⁺CD45RA⁺, and memory CD4 was CD4⁺CD45RA⁻. The memory CD4 was then further divided into several subsets, including central memory (CD4⁺CD45RA⁻CCR7⁺CD28⁺), effector memory (CD4⁺CD45RA⁻CCR7⁻CD28^{+/-}) and terminally differentiated memory (CD4⁺CD45RA⁻CCR7⁻CD28⁺). In this assay, each of the antibodies were conjugated with one specific fluorescence, including CD4-FITC, CD45RA-PerCP710, CD57-APC (Biolegend, San Diego, CA), CD28-PE (Invitrogen, Carlsbad, CA), PD1-FITC (eBioscience, San Diego, CA).

Cell Apoptosis Qualification

Apoptosis, also called programmed cell death, is a normal cellular process where cells are induced to die in order to maintain an appropriate cell population during development and aging. It also serves as an immune defense when cells are under attack by pathogens, noxious agents, or diseases. At certain conditions, cells are marked with apoptosis markers and induced to go under apoptotic pathways which eventually results in self-destruction without affecting other adjacent cells. Apoptosis and necrosis, a process in which the cells are forced to die under physical or chemical pressures, are easy to be mistaken for each other, since both processes induce cell deaths. Both of the processes can occur independently, sequentially, or even simultaneously. The key difference between them is the way the cells die. When induced by apoptosis, cells die by cell shrinkage; therefore, it does not release its cytoplasmic content into the surrounding environment and later will be phagocytosed by macrophages or the adjacent cells without causing inflammation reactions. Opposite to this mechanism, cells induced by necrosis die by bursting and releasing its cytoplasmic content, which can lead to a domino effect of inflammation to the whole tissue or organ. The specific morphologies of apoptotic cells are cell shrinkage, membrane blebbing, chromosome condensation, nuclear fragmentation, and DNA laddering. Apoptosis is considered as an irreversible process by which caspase activation leads to cell suicide³⁴.

There are three pathways involved in cell apoptosis, including the extrinsic or death receptor pathway, intrinsic or mitochondrial pathway, and perforin/granzyme pathway. These three pathways are stimulated by different stimuli and have several distinguishable proteins involved. However, they eventually lead to the activation of a common protein kinase called caspase-3, which initiates the executive apoptotic pathway that leads to cell death. The stimuli of

the extrinsic pathway are death ligands, such as Fas. When bound to its receptor, Fas can activate the adaptor protein called FADD, meanwhile, the binding of TNF ligand to its receptor activates that TRADD protein. This protein then recruits the binding of FADD and RIP proteins, then the complex comes to have an association with procaspase 8 forming death-inducing signaling complex (DISC) which in turn phosphorylates the caspase-3 protein. The perforin/granzyme pathway is stimulated by viral infections or tumors and induced under cytotoxic T cell signaling. When stimulated, T cells exert its cytotoxic effects on targeted cells via a pathway involving the secretion of transmembrane pore-forming molecules called perforin together with cytoplasmic granules such as granzyme A or granzyme B. These proteins can act as endonucleases that cleave proteins into fragments which can later activate the caspase-3 protein. There are a wide range of stimuli that can the activate apoptotic intrinsic pathway, including radiation, hypoxia, viral infection, or free radicals. These stimulations cause the opening of mitochondria permeability transition pore, resulting in the loss of membrane potential which leads to the leaking of the lumen content, including cytochrome c. Cytochrome c is well known for its function in cellular respiration inside the lumen of mitochondria; however, when released into the cytoplasm, it forms a complex with Apaf-1 and procaspase 9 to form apoptosome, which will later trigger the cascade activations of caspase 9 and caspase-3. As mentioned above, all three apoptosis pathways lead to the activation of caspase-3, which can phosphorylate CAD endonuclease that cleaves proteins such as cytokeratin or PARP. These proteins can cause cellular morphological and biochemical changes, eventually leading to cell death³⁵⁻³⁶.

Currently in scientific research, there are three assays heavily used for the detection of apoptotic markers by FCM, including Annexin/7-AAD (BD PharmingenTM PE Annexin V Apoptosis Detection Kit I, BD Biosciences, San Jose, CA), and measurement of reactive oxygen

species (ROS) (DCFDA-based Cellular ROS Detection Kit, Abcam, Cambridge, MA). One of the biochemical features of early apoptosis is the externalization of phosphatidylserine, a component of plasma membrane normally inward-facing, to be expressed on the outer layers of plasma membrane. This phospholipid therefore acts as a ligand for the phagocytosis signaling of adjacent cells to digest the phosphatidylserine expressing cells. Because of its feature, phosphatidylserine is immensely used as a marker for apoptosis. Annexin V, a recombinant protein that strongly and specifically binds to phosphatidylserine, together with 7-AAD which is a fluorescent DNA binding dye indicating the membrane impermeability, can be used to identify the apoptotic cells at different states. Cells that stained positive for Annexin V and negative for 7-AAD are considered to be in early apoptosis. Cells that stained both positive for Annexin V and 7-AAD are either at the end stage of apoptosis or already in death. Cells that stained negative for both the reagents are alive and not undergoing measurable apoptosis³⁷. Another method to track the apoptotic cells is to measure the activated caspase-3 by using fluorescently conjugated antibody against it. This can be achieved by performing intracellular FCM staining³⁸. The last assay used in apoptosis identification is ROS detection. ROS are short-lived and highly reactive molecules that play essential roles in cell development such as differentiation, proliferation, cell signaling, and immune defense. However, when there is an imbalance in ROS generation and antioxidant to neutralize it, ROS can cause serious cellular damages, including damage to protein, DNA, lipid, and organelles. Since ROS are a type of free radical, its excessive level can trigger the activation of intrinsic apoptosis pathway³⁹.

Analysis of Interest Proteins

The interest protein expressions were measured both in qualification and quantification by intracellular staining by FCM, including phosphorylated ATM (pATM) at serine 1981 with

PE fluorescence (BioLegend), and phosphorylated CHK2 (pCHK2) at threonine 68 with PE fluorescence and γ -H2AX-PE (eBioscience).

FCM Detailed Protocols

Extracellular staining. Cultured cells were harvested and washed with cell staining buffer by centrifugation at 1200 rpm for 5 minutes, followed by removal of the supernatant. The cell pellet was resuspended with 50 μ l of staining buffer in a 2ml centrifugation tube. The mixture was then incubated with 1 μ l of fluorescence-conjugated antibody for 20 minutes at room temperature, light avoided. After the incubation, the tube was centrifuged at 1200 rpm for 5 minutes, the supernatant was discarded, and the cell pellet was resuspended with 50 μ l staining buffer and ready to be analyzed by FCM.

Intracellular staining. Cultured cells were harvested and washed with cell staining buffer by centrifugation at 1200 rpm for 5 minutes, followed by removal of the supernatant. The cells were then fixed by being resuspended with 100 μ l diluted formalin solution and incubated in the dark at room temperature for 60 minutes. The mixture was then centrifuged at 1200 rpm for 5 minutes and the supernatant was removed. The cell pellet was resuspended with 2ml of permeabilization buffer and centrifuged again at 1200 rpm for 5 minutes. The supernatant was discarded. The cell pellet was then mixed with 100 μ l permeabilization buffer and 2 μ l of fluorescence-conjugated antibody, then the mixture was incubated in the dark at room temperature for 60 minutes. The cell pellet was obtained by centrifugation after the incubation, then resuspended with 100 μ l of staining buffer and ready for FCM analysis.

Annexin V/7-AAD staining assay. Cultured cells were harvested and washed with cell staining buffer by centrifugation at 1200 rpm for 5 minutes, followed by removal of the. The cell

pellet was then resuspended with Camptothecin (already diluted with DMSO) and incubated at 37°C in 6 hours. After the incubation, the cells were washed twice with cold PBS and then resuspended in 1X binding buffer at a concentration 1×10^6 cells/ml. 100µl of the mixture was then transferred into new tube and 5µl of Annexin V and 5µl of 7-AAD were added. The tube was then incubated in the dark at room temperature for 15 minutes. After the incubation, 400µl of 1X binding buffer was added and then the cells were ready for FCM analysis.

ROS detection assay. The principle of this assay is to measure the concentration of 2', 7'- dichlorofluorescein (DCF). The beginning reagent is 2', 7'- dichlorofluorescein diacetate (DCFDA). After diffusion into the cell, DCFDA is deacetylated by cellular esterase to a non-fluorescent compound, which is later oxidized by ROS into DCF. DCF is a highly fluorescent compound which can be measured by FCM. Cultured cells were harvested and washed with cell staining buffer by centrifugation at 1200 rpm for 5 minutes, followed by removal of the. The cell pellet was then resuspended with culture media and incubated with 20µM DCFDA for 30 minutes in the dark at 37°C. After the incubation, the cells were analyzed by FCM. In this assay, tert-butyl hydrogen peroxide (TBHP) was used as positive control. TBHT was prepared by diluting 55mM TBHT stock solution in 1X supplemented buffer to achieve 50-250µM concentration. The positive control was incubated for 4 hours in the dark at 37°C before FCM analysis.

Flow-FISH

Flow-FISH (fluorescent in-situ hybridization) is a cytogenetic technique used for quantifying the copy number of specific repetitive element in genomic DNA by the combination of the two techniques in which the staining protocol is based in FISH and the copy number is analyzed by FCM. This technique is mostly used to determine telomere length in scientific

research. The principle of this technique is using a labelled probe able to hybridize to telomere repeats in the cell suspension. The telomere length is estimated based on the average fluorescent signals quantified by FCM. The fluorescence-conjugated probe used in this assay is a peptide nucleic acid (PNA) in which the sugar backbone has been replaced by a neutral peptide-polyamide backbone. This backbone is highly resistant to the degradations caused by endonucleases such as DNase, RNase, protease, or peptidase, which makes it more stable in the cell lysate. Another crucial characteristic of this probe is its high affinity and high specificity binding to its target DNA sequence, which makes it an ideal tool for the analysis ⁴⁰.

The general protocol used in our project was modified from Flow-FISH method as previously described. Isolated PBMCs were stained with CD4-A647 and fixed with cell fixation buffer (BioLegend) for 20 minutes at room temperature. After being fixed, the cells were incubated with telomere PNA probe TelC (CCCTAACCCCTAACCCCTAA)-FITC in which the concentration is 0.3µg probe/mL (PNA Bio, Newbury Park, CA) at room temperature for 10 min in the dark. After that, the cells were incubated at 82°C for another 10 minutes. After the incubation, the cells were washed with post-hybridization buffer, followed by flow cytometry buffer, and then stained with CD45RA-perCP/Cy5.5 and analyzed by flow cytometry.

Confocal Microscopy

Confocal microscopy is an optical imaging technique that can enhance the visualization of biological samples by capturing the images at different depths and enable the three-dimensional reconstruction of the samples. In this project, confocal microscopy is combined with immunofluorescence, a technique used in detection of proteins using fluorescently conjugated antibodies, in order to determine the telomere function by identifying the localization of telomere

associated proteins and DDR proteins to form DNA damage foci. As mentioned in the introduction, telomeres are protected by shelterin which consists of six proteins. When DNA damage occurs at the telomere, DDR is triggered and proteins involved in this pathway are recruited to the DNA damage sites. Therefore, there must be interactions between the shelterin complex and DDR pathway. These associations are called DNA damage foci and are considered as DNA damage markers. In this project, the DNA damage foci formed from the associations of 53BP1, which belongs to the DDR pathway and has binding domains for both p53 proteins and modified histone conformations, and TRF1 proteins was used as the telomeric DNA damage evaluation. The principle of the procedure is that the permeabilized cells were incubated with primary antibodies against 53BP1 and TRF1 proteins, followed by the incubation of secondary fluorescent conjugated antibodies and visualized by confocal microscopy.

The general protocol was described previously. In brief, cultured cells were harvested and washed with cell staining buffer by centrifugation at 1200 rpm for 5 minutes, and the supernatant was then removed. The cell pellet was then mixed and fixed by 2% paraformaldehyde solution for 20 minutes, followed by cell permeabilization by 0.3% triton X 100 in PBS for 10 minutes. After that, the cells were blocked with 5% bovine serum albumin (BSA) in PBS for 1 hour. Then the cells were incubated with the primary antibodies against 53BP1 (Cell Signaling) and TRF1 (Thermo Fisher) at 4°C overnight. After the incubation, the cells were washed with PBS containing 0.1% Tween solution for three times before being incubated with secondary fluorescence-conjugated rabbit antibody in the dark for 1 hour. Then, cells were washed with PBS and mounted with DAPI fluoromount-G (SouthernBioTech, Birmingham, AL), which is an impermeant plasma membrane dye. Finally, cells were visualized under confocal laser-scanning inverted microscope (Leica Confocal, Model TCS sp8, Germany).

RNA Isolation and Real-time RT-PCR

In scientific research, the quantity of gene expression is mostly achieved by performing RNA isolation followed by the real-time reverse transcription polymerase chain reaction (RT-PCR) technique. Following the central-dogma flow of genetic information, it is known that the term gene expression is preferred to the order of processes which include the transcription of RNA based on the DNA sequence and then the translation of protein based on the order of nucleic acids present on the transcribed RNA. Therefore, gene expression level can actually be measured by the quantification of transcribed RNA levels. Currently, there is no efficient method to measure the level of RNA expression; therefore, RNA is usually converted back into complementary DNA (cDNA) by RT-PCR, which can be tagged with fluorescence, then amplified and quantified by real-time RT-PCR.

The total RNA was isolated using the RNeasy Mini Kit (Qiagen). Cultured cells were harvested and washed with cell staining buffer by centrifugation at 1200 rpm for 5 minutes, and the supernatant was then removed. Then the cells were disrupted by RTL buffer (supplied) so that 300 μ l buffer was used for each of 5×10^6 cells. Then the cell lysate was homogenized by being vortexed for 1 minute. Then 1 volume of cold 70% ethanol was added into the tube containing cells, and mixed well. After that, the mixture of approximately 700 μ l was transferred to RNeasy spin column placed on 2ml collection tube (supplied), which was then centrifuged at 10000 rpm for 15 seconds. The flow through solution was discarded. After that, 700 μ l RW1 buffer (supplied) was added into the column followed by a centrifugation at 10000 rpm for 15 seconds, the flow through was discarded. In the next step, 500 μ l of RPE buffer (supplied) was added into the column and centrifuged at 10000 rpm for 15 seconds, the flow through was discarded. This step was repeated one more time in which the centrifugation time was 2 minutes.

The column was then placed onto a new 1.5ml collection tube (supplied) and added with 30 μ l of RNase-free water (supplied) and centrifuged for 1 minute at 10000 rpm to elute the total RNA.

The master mix solution was prepared by adding the reagents supplied with appropriate concentrations listed in the table 1 below. CDNA was synthesized using High Capacity cDNA Reverse Transcription Kit (Applied Bio systems, Fostercity, CA). The concentration of isolated total RNA was up to 2 μ g per 20 μ l reaction.

Table 1: List of PCR Master Mix Components and Concentrations

Components	Volume/Reaction (μ l)
10X RT buffer	2.0
25X dNTP Mix (100mM)	0.8
10X RT Random Primers	2.0
MultiScribe TM Reverse Transcriptase	1.0
RNase Inhibitor	1.0
Nuclease-free H ₂ O	3.2
Total per Reaction	10.0

The cDNA RT reaction was prepared by mixing 10 μ l of master mix and 10 μ l of total RNA in each of the individual tubes. Then the tubes were briefly centrifuged and placed into the thermos cycler. The thermo cycler conditions were programed as listed in table 2.

Table 2: cDNA Synthesis Thermo Cycler Conditions

	Step 1	Step 2	Step 3	Step 4
Temperature (°C)	25	37	85	4
Time (minute)	10	120	5	∞

The purpose of the real-time RT-PCR technique is to amplify DNA using cDNA sequences as templates and to quantify the gene expression level based on the measurement of fluorescent signals. The DNA-binding dye used in this technique is called SYBR Green I (Bio-rad Laboratories, Philadelphia, PA), which binds nonspecifically to double-stranded DNA. This probe exhibits little green fluorescence in its free form, but when bound to double-stranded DNA, its fluorescence increases significantly and is detected by the machine linked with computer analysis. Therefore, the intensity of fluorescent signal released during real-time RT-PCR reaction is proportional to the amount of DNA amplified, which in turn is equivalent to the level of mRNA presented.

In order to perform the experiment, master mix was prepared by mixing 10 μ l of SYBR Green I, 8 μ l distilled water, 1 μ l of forward primer and 1 μ l of reverse primer for each of the reactions. The primer was diluted before used so that its final concentration was 5 μ M/ μ l. Then the mix was placed into a 96-well PCR plate and the plate was sealed and placed into the thermos cycler, which was programed following the conditions listed in table 3 below. The house keeping control used in this assay was GAPDH. The primers used are listed in table 4 below. All of the primers were customized by Thermo Fisher. Gene expression was normalized to GAPDH and values are expressed as fold changes using the $2^{-\Delta\Delta CT}$ method.

Table 3: Real-time RT-PCR Thermo Cycler Conditions

	Step 1	Step 2	Step 3	Step 4
Temperature (°C)	95	95	60	60
Time/cycle	10 min	5 min	60 sec	40 cycles

Table 4: List of Primers used in the Study

Genes to be amplified	Primer sequences
ATM	F: 5'-TGGATCCAGCTATTTGGTTTGA-3'
	R: 5'-CCAAGTATGTAACCAACAATAGAAGAAGTAG-3'
MRE11A	F: 5'-CTTGTACGACTGCGAGTGGA-3'
	R: 5'-TTCACCCATCCCTCTTTCTG-3'
RAD50	F: 5'-CTTGGATATGCGAGGACGAT-3'
	R: 5'-CCAGAAGCTGGAAGTTACGC-3'
NBN	F: 5'-TTGGTTGCATGCTCTTCTTG-3'
	R: 5'-GGCTGCTTCTTGGACTCAAC-3'
CHEK2	F: 5'-CCCAAGGCTCCTCCTCACA-3'
	R: 5'-AGTGAGAGGACTGGCTGGAGTT-3'
TP53	F: 5'-TCAACAAGATGTTTTGCCAACTG-3'
	R: 5'-ATGTGCTGTGACTGCTTGTAGATG-3'
GAPDH	F: 5'-TGCACCACCAACTGCCTTAGC-3'
	R: 5'-GGCATGGACTGTGGTCATGAG-3'

Western Blotting

Western Blot, also called immunoblotting, is a widely used technique for detection and characterization of proteins. The technique principle is based on immunochromatography where proteins are separated according to their molecular weights by gel electrophoresis. The separated proteins are then transferred and immobilized onto a nitrocellulose membrane where they will be bound with primary, then secondary antibodies and detected by chemiluminescence. This study used the Amersham ECL Prime Western Blotting Detection Reagent (GE Healthcare Bio-Sciences, Pittsburgh, PA). The western blot protocol consists of five main steps, including protein purification, gel electrophoresis, membrane transferring, antibody incubation, and protein detection.

The protein purification step begins by cell harvesting. Cultured cells were harvested and washed with cell staining buffer by centrifugation at 1200 rpm for 5 minutes, followed by removal of the. The cell pellet was suspended with homogenization buffer containing no SDS RIPA buffer (Thermo Fisher) and 1X protease inhibitor. Then the tube containing the mixture was vigorously vortexed for 30 seconds, placed on ice for 5 minutes, shaken for 10 minutes at 4°C, and finally was centrifuged at 13000 rpm at 4°C for 15 minutes. The supernatant, which was protein mixture, was collected and transferred into a new tube.

The purified proteins were separated by gel electrophoresis. The resolving gel was prepared by adding the appropriate amount of reagents listed in table 5 and stacking gel in table 6 below. The prepared gel was placed into the chamber which contained 1X running buffer (Bio-Rad Laboratories). The chamber was then connected to the electronic machine, the gel was run under the two steps protocol. In step 1, the gel was run under 75V for 80 minutes and in step 2, it was 125V for 45 minutes.

Table 5: Western Blotting Resolving Gel Preparation Components

	8%	10%	12%
Water (mL)	4.6	3.8	3.2
30% acrylamide (mL)	2.6	3.4	4.0
1.5M Tris – HCL, pH 8.8 (mL)	2.6	2.6	2.6
10% SDS (μL)	100	100	100
10% APS (μL)	100	100	100
TEMED (μL)	10	10	10

Table 6: Western Blotting Stacking Gel Preparation Components

	5%
Water (mL)	5.86
30% acrylamide (mL)	1.34
1.5M Tris – HCL, pH 8.8 (mL)	2.6
10% SDS (μL)	100
10% APS (μL)	100
TEMED (μL)	10

After the separation, the proteins were then transferred onto nitrocellulose membrane when the gel and membrane were placed together in the transfer chamber containing transfer buffer, made by mixing 10X transfer buffer, methanol and distilled water in the ratio of 1:2:7, respectively. The chamber was connected to the electronic machine, which was set at 30V and the transfer process took place in the cold room overnight.

The next morning, the membrane was blocked with 5% skim milk in tris-buffered saline containing tween (TBST) at room temperature for an hour, then washed three times with TBST. After that, the membrane was incubated with primary antibody in BSA solution, in which the antibody was diluted 1:1000, overnight in the cold room. In the next step, the membrane was washed three times with TBST, then incubated with secondary antibody for 1 hour at room temperature. After the incubation, the membrane was again washed three times with TBST, then it was dropped with chemiluminescence solution for 5 minutes and detected by Chemi Doc™ MP Imaging System (Bio-Rad System). All of the antibodies were purchased from Cell Signaling. The house keeping protein used in this study was β -Actin.

Statistical Analysis

The data was analyzed using Prism 7 software and are presented as mean \pm SEM or median with interquartile range. Differences between two groups were analyzed by independent Student's *t* test or Mann Whitney test, paired T test, or Wilcoxon matched-pairs signed rank test. Multiple groups were analyzed by one-way ANOVA test. P-values <0.05, <0.01, or <0.001 were considered statistically significant or very significant, respectively.

Experimental Design

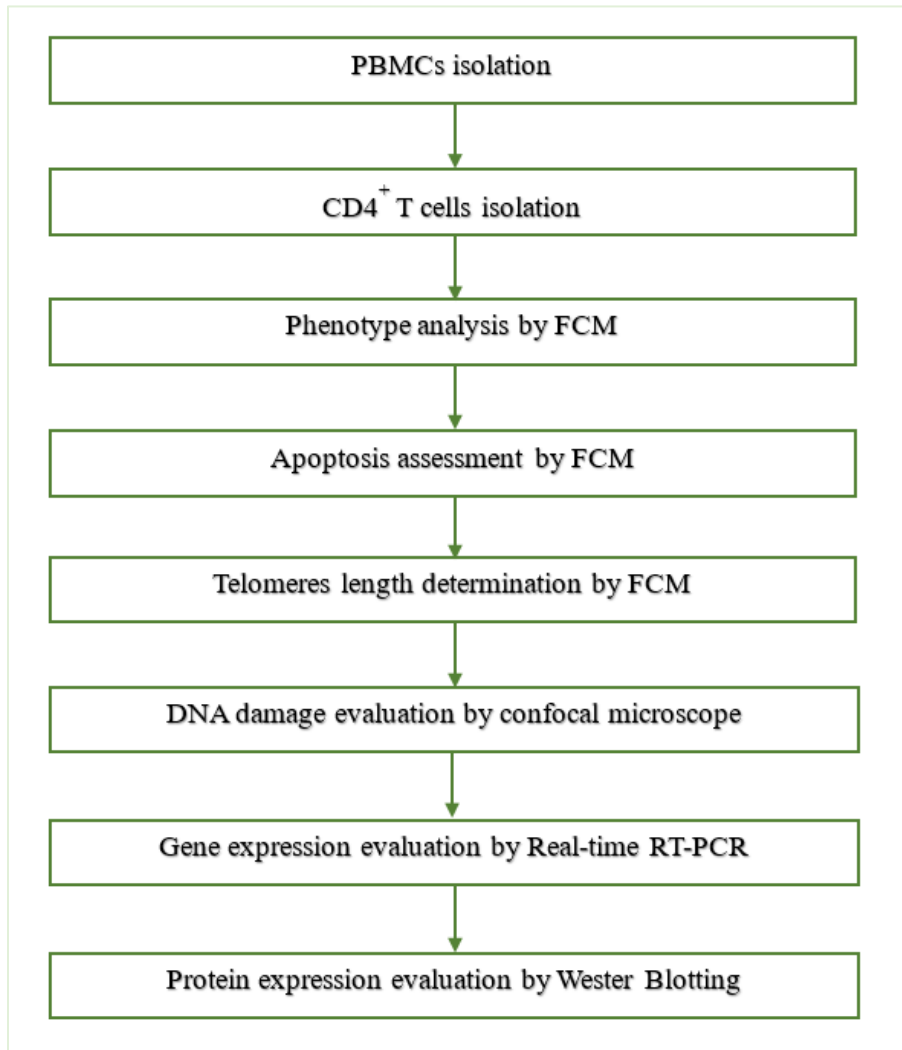


Figure 1: Experimental design

The general workflow of the study is described in Figure 1. First of all, human whole blood was collected from chronically HIV-infected patients and healthy subjects. PBMCs were isolated by density-gradient centrifugation. In the next step, the isolated PBMCs were used as the source for further purification of total CD4T cells using the CD4T cell isolation kit, which includes antibody cocktail and microbeads cocktail and LS column for magnetic separation.

Isolated CD4T cells were cultured with RPMI 1640 complete media for 4 days in the incubator hood. Cells were then harvested and taken for further assays. The first assay was the phenotype analysis of CD4T cell populations by FCM. The second one was the assessment of cellular apoptosis using FCM. The next assay performed was DNA damage determination by immunofluorescence and confocal microscope. After that, telomere length was determined by FCM analysis. Gene expression of proteins involved in the ATM-p53 DDR pathway and shelterin complex were evaluated by RNA extraction, cDNA synthesis, and real-time RT-PCR. Last but not least, the expression levels of those proteins were estimated by western blotting.

The data collected after these assays will be analyzed and compared between Healthy and HIV-infected subjects using unpaired t-test. If the p value is smaller than 0.05 or even < 0.001 , then the results between the two groups are regarded having significant or very significant difference; otherwise, the two groups do not have a significant difference.

CHAPTER 3

RESULTS

CD4T Cells Homeostasis and Apoptotic Susceptibility in Latently HIV-infected Individuals on ATR Treatment

As mentioned by previous studies, T cell dysregulation is a specific characteristic caused by chronic viral infections, including HIV infection. However, the detailed mechanism by which viral infections persistently trigger the response of immune system, eventually resulting in the loss of T cell homeostasis, still remains unclear. In order to determine the characteristics of T cells in latently HIV-infected patients, T cell phenotypic analysis by FCM was performed with the collected data in Figure 2, which is a representative dot plot and summary data from FCM analysis. In this assay, the number of lymphocytes, including total CD4⁺, naïve CD4⁺CD45RA⁺ and memory CD4⁺CD45RA⁻ helper T cells present in PBMCs of HIV-infected patients (n=24) and age-matched healthy subjects (n=27) was determined. As shown in the figure, the percentages of these cells in PBMCs of HIV-infected patients were significantly less than healthy subjects, in which the differences of total CD4 (p=0.0001) and memory CD4 (p=0.0001) were considered very significant with small p values. In addition, naïve CD4 were also considered to be significant with p=0.043. The percentages of memory CD4T cells, including central memory (CD4⁺CD45RA⁻CCR7⁺CD28⁺), effector memory (CD4⁺CD45RA⁻CCR7⁻CD28^{+/-}) and terminally differentiated memory (CD4⁺CD45RA⁻CCR7⁻CD28⁺) were further investigated. The results indicated that all three subpopulations of memory CD4T cells were significantly decreased in HIV-infected patients compared to healthy subjects. Among those, central memory CD4 cells had the most significant difference (data not shown). The contractions of CD4T cells, especially central memory CD4T cells in HIV-infected individuals compared to

healthy subjects, are consistent with previous reports which indicated that T cells are exhausted and senescent in latent HIV infected individuals.

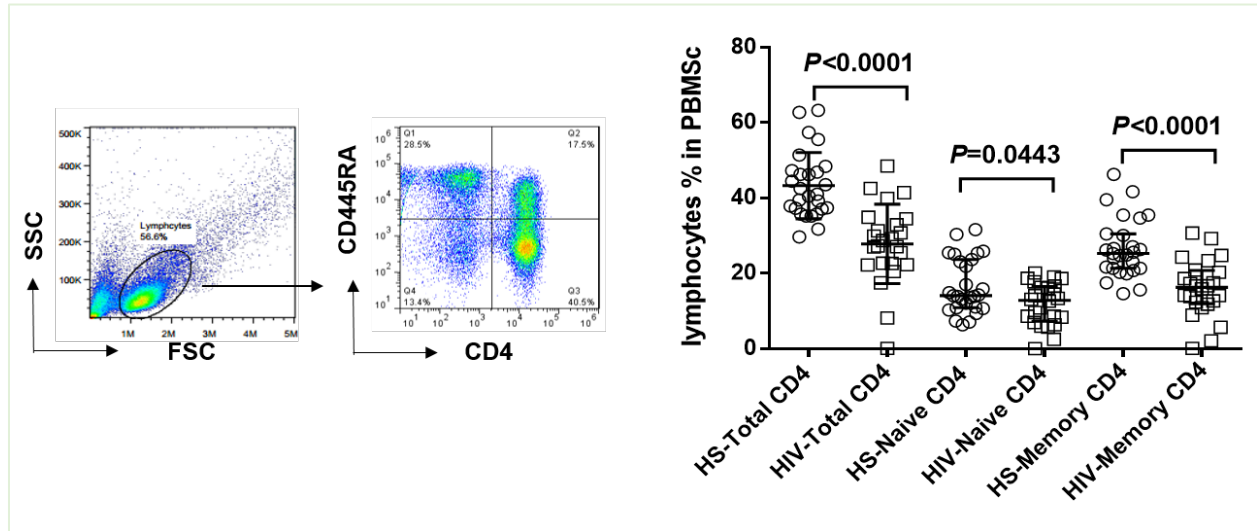


Figure 2: Percentage of lymphocytes in PBMCs analyzed by FCM. PBMCs were isolated from 24 HIV-infected patients and 27 healthy subjects analyzed for T cell homeostasis by FCM. Representative dot plots and summary data for the homeostasis of T cell populations are shown. Total CD4T cells were defined as $CD4^+$, naïve CD4as $CD4^+CD45RA^+$ and memory CD4as $CD4^+CD45RA^-$. Each dot represents an individual. The means, \pm SD and p values are also shown.

The T cells repertoire in PBMCs is well balanced between the number of newly synthesized T cells and the number of dying T cells via programmed cell death or their engagement with pathogens, within the existing T cell population. Chronic viral infection usually triggers the central memory CD4T cells to produce more and more effector CD4cells to suppress the viral concentration. Long term, the continuous generation of effector T cells by central

memory T cells leading to proliferative turnover, causes loss of homeostasis, telomere erosion, and ultimately, cellular apoptosis. In order to determine the apoptosis level in CD4T cells, these cells were stained with apoptotic markers Annexin V and 7-AAD and analyzed by FCM analysis, the collected data is shown in Figure 3.

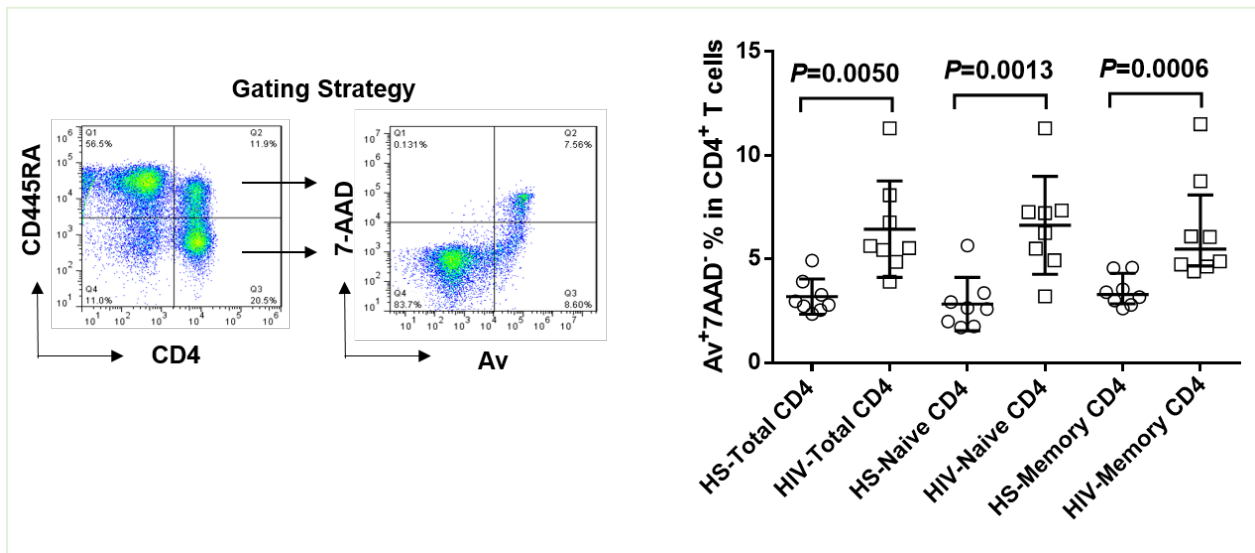


Figure 3: The percentage of Av⁺/7-AAD positive CD4 populations. PBMCs from 8 individuals of each HIV-infected and healthy subject groups were isolated and analyzed by FCM analysis. Representative dot plots and summary data for percentage of Av⁺/7-AAD expression in CD4populations. Total CD4T cells were defined as CD4⁺, naïve CD4as CD4⁺CD45RA⁺ and memory CD4as CD4⁺CD45RA⁻. Each dot represents an individual. The means, \pm SD and p values are also shown.

It can be observed that, the expressions of early apoptotic markers were significantly higher in all subpopulations of CD4T cells in HIV-infected patients compared to healthy subjects. The p values were $p=0.0050$, $p=0.0013$ and $p=0.0006$ for total, naïve and memory

CD4T cells, respectively. In order to evaluate the correlation between T cell exhaustion and cellular apoptosis, the data collected by FCM was then further analyzed by Pearson Correlation (PC) analysis. Figure 4 shows a negative correlation between the percentage of total and memory CD4T cells in PBMCs and the level of cellular apoptosis in HIV-infected patients, in which the lower the concentration of CD4T cells, the higher the apoptotic marker expressions are and vice versa, with $r=-0.4416$, $p=0.0868$ and $n=8$ for each HIV-infected and healthy subjects.

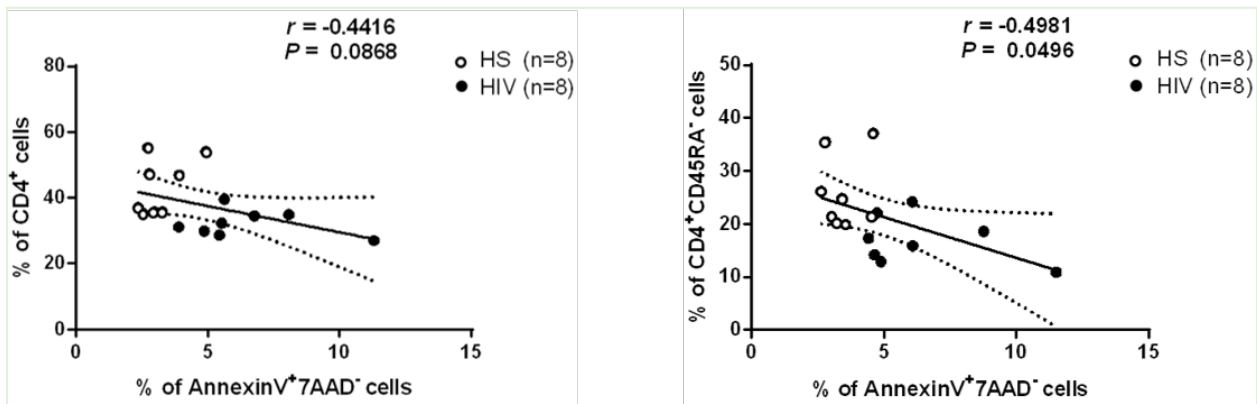


Figure 4: The Pearson Correlation analysis between percentage of CD4T cells and apoptosis. PBMCs from 8 individuals of each HIV-infected and healthy subject groups were isolated and analyzed by FCM analysis.

In addition, FCM data analyzed by PC analysis in Figure 4 also showed that there was a positive correlation between the percentage and the actual counts of CD4 cells. The above data suggests a close correlation between T cell exhaustion and cellular apoptosis, in which individuals infected with HIV had low CD4T cell number and high apoptotic marker expressions.

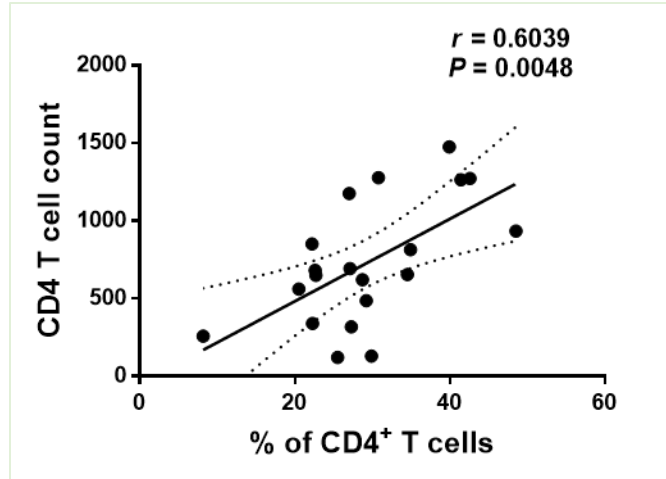


Figure 5: The Pearson Correlation analysis between percentage of CD4T cells and the actual CD4T cell counts in HIV infected-patients. The r and p values are shown in the figure.

CD4 T cell Exhaustion and Senescence in Latent HIV Infection

To further characterize the T cell exhaustion and senescence in latent HIV infection, we further investigated the expressions of relevant markers in both HIV-infected patients and age-match healthy subjects by FCM analysis. The first marker used was programmed cell death 1 protein (PD1), which was considered as marker of T cell exhaustion. As showed in Figure 6, the expression of this protein was significantly higher in HIV-infected patients when compared to healthy subjects both in lymphocyte population with $p=0.0055$, and CD4T cell alone with $p=0.0231$. On the other hand, the expressions of PD1 protein in CD4T cells who were at resting state, as well as those in CD8⁺ T cells, were comparable to healthy subjects (data not shown).

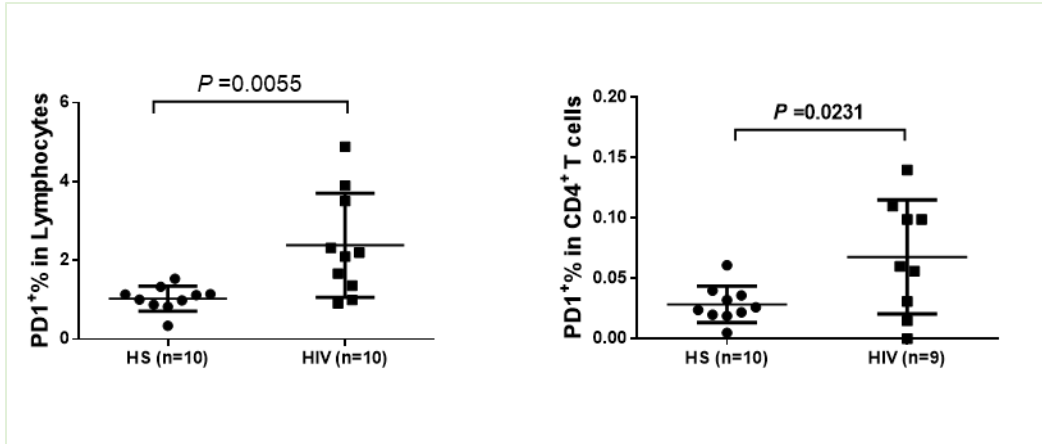


Figure 6: Percentage of PD1 protein in lymphocytes and CD4 T cells analyzed by FCM analysis. Lymphocytes and total CD4T cells were isolated and analyzed by FCM for PD1 determination. Each dot in the figure represents an individual. The means, \pm SD and p values are also shown.

The next relevant marker used for comparison between HIV-infected patients and healthy subjects was CD28 protein, a co-receptor necessary for T cell activation and survival. Therefore, the loss of this protein is equivalent to T cell senescence. However, as shown in Figure 7, there was no significant difference in the expression of this marker in CD4T cells in HIV-infected patients compared to healthy subjects. Another marker evaluated was CD57 protein, which is considered as the specific marker for a subset of T lymphocytes called natural killer cells. Besides its well-known role, CD57 protein has been considered to represent a marker for T cell exhaustion. It can be observed in Figure 7, there was a significant difference in the expression of CD57 protein in HIV-infected patients and healthy subjects, in which there was a much higher concentration of this protein found on the membrane of HIV-infected patients' T cells, $p=0.0059$. This data suggested that chronic HIV-infection causes cellular exhaustion and senescence in T lymphocytes, especially in the CD4 population.

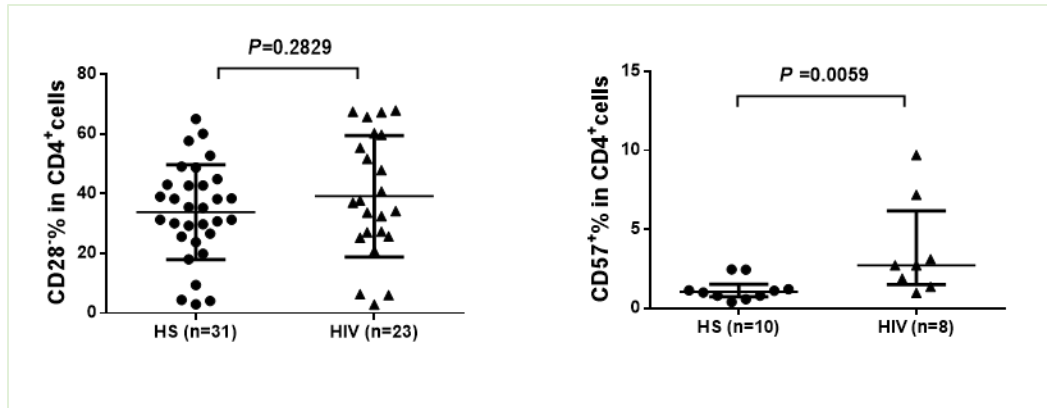


Figure 7: The percentage of CD28 and CD57 protein expressions in CD4T cells analyzed by FCM. The number of individuals in each HIV-infected and healthy subject groups are shown. Each dot in the figure represents an individual. The means, \pm SD and p values are also shown.

Telomere Attrition and Telomeric DNA Damage in CD4 T Cells during Latent HIV Infection

The importance of telomere function was mentioned in the introduction since telomeres, together with its associated proteins, act as a shield to protect genome stability from DNA damage and to prevent cellular senescence. Without their protection, the genomic integrity would be corrupted and result in serious diseases. To further investigate the telomere function and the wealth of telomeric DNA in latent HIV infection, telomere lengths of HIV infected individuals and healthy subjects were measured by FCM analysis using the median fluorescence intensity (MFI) generated from the fluorescent signal of telomeric DNA complementary probes. The higher the MFI, the longer the telomere length. Collected data is represented in Figure 8, which showed that the telomere length of CD4T cell populations in HIV-infected patients was shorter than for healthy subjects. Among those, telomere lengths of total and memory CD4T cells from HIV-infected patients were significantly lower with $p=0.0423$ and $p=0.0260$, respectively.

However, there was no significant difference in the telomere length of naïve CD4 population between the two groups ($p=0.1467$).

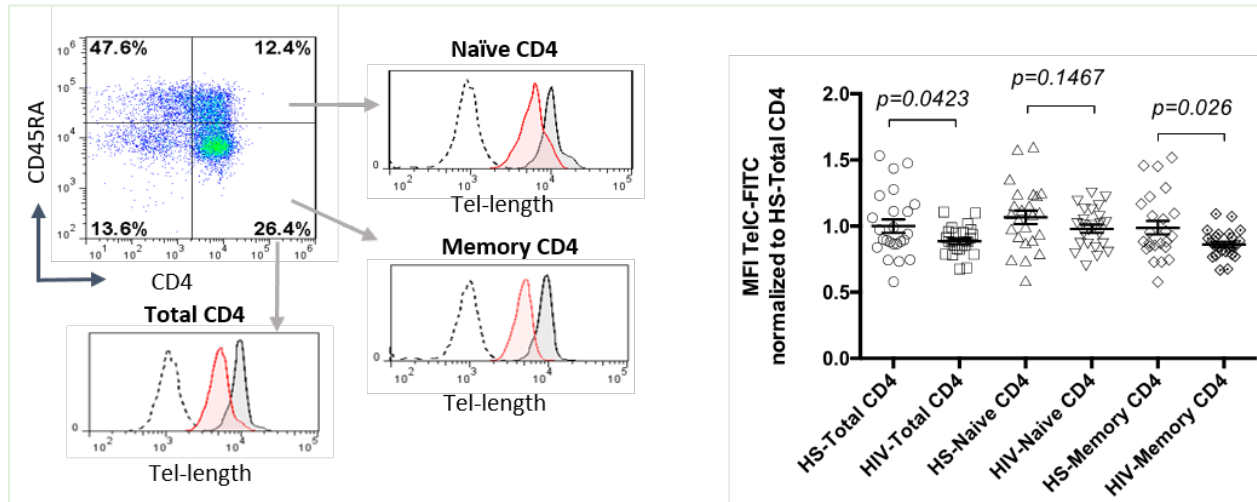


Figure 8: Telomere length determination by Flow-FISH analysis. CD4T cells from 24 samples from each of HIV-infected patient and healthy subject groups were isolated and had their telomere length determined by Flow-FISH analysis. Representative dot plots, summary data, and flow cytometry histogram are shown. Each dot in the figure represents an individual.

The means, \pm SD and p values are also shown.

More importantly, when the cells were measured for both telomere length MFI and cellular apoptosis markers, Annexin V and 7-AAD, PC data analysis indicates, as shown in Figure 9, a negative correlation between cellular apoptosis and telomere length in HIV-infected patients, with $r=-0.3318$ and $p=0.0212$. It can be observed that the shorter the telomere length, the higher cellular apoptosis.

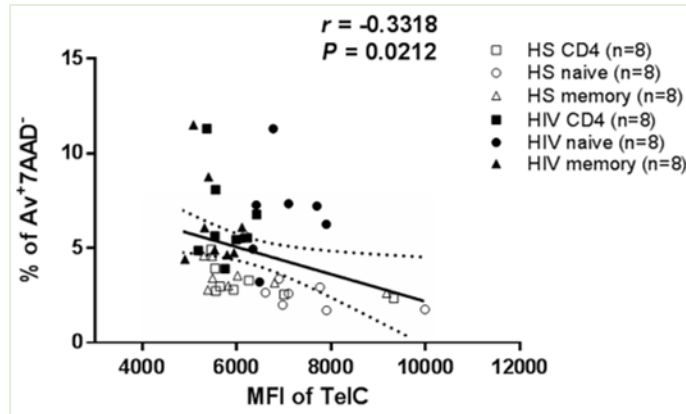


Figure 9: Pearson correlation analysis of the telomere length (MFI) and the percentage of early apoptotic cells. The r and p values are shown in the figure.

CD4 T cell Exhaustion and Senescence in Latent HIV Infection

This data indicated that telomere erosion is closely associated with apoptosis in latent HIV infection. In addition, it also raised a question regarding the unknown mechanism or pathway causing telomere shortening and cellular apoptosis in latent HIV infection while the patients were under ART treatment with undetectable viral load in their blood. One of the possible explanations is the increase in concentration of reactive oxygen species (ROS), a substance which plays important roles in many cellular processes at appropriate concentration. The excess amount of ROS could cause extreme harm to cellular health, such as oxidative stress. In order to test this hypothesis, the level of ROS present in HIV-infected patients and healthy subjects was measured using Cellular ROS Detection Kit based on the absorption of DCFDA which can be bound with cytochrome c enzyme, a protein involved in cellular respiration together with the release of ROS substance via the process. As shown is Figure 10, the level of DCFDA signal generated by HIV-infected patients was higher when compared to healthy

subjects in cells cultured for 1 day ($p=0.0939$) and significantly higher in cells cultured for 4 days ($p=0.0035$), indicating there was a higher ROS concentrations in HIV-infected individuals.

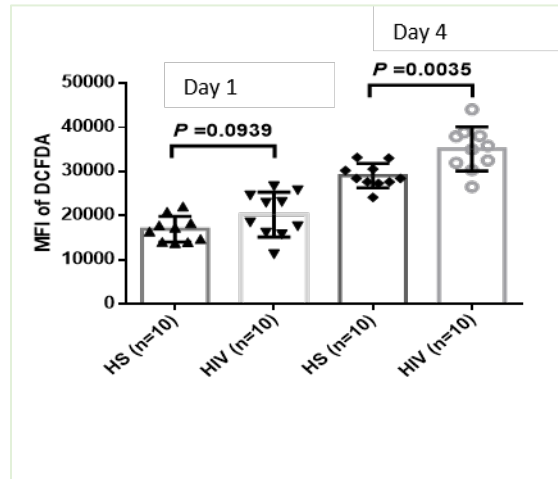


Figure 10: Median Fluorescence Intensity of DCFDA in HIV-infected patients and healthy subjects. CD4T cells of 10 individuals from each group were isolated and determined for the MFI of DCFDA by FCM analysis. Each dot in the figure represents an individual. The means, \pm SD and p values are also shown.

However, because the principle in measuring ROS of this kit is based on the level of cytochrome c, which is usually through the mitochondrial membrane into cytosol during apoptosis, it is dependent on the apoptosis pathway and it could not tell us whether ROS, independent of the apoptosis pathway, actually have any impact on the telomere erosion and trigger the apoptosis or not. Because of that, another ROS measuring method was used, called CellROX Green kit, which actually forms direct binding with ROS substances. In this experiment, cells from HIV-infected patients and healthy subjects were stained with both

CellROX green fluorescence and apoptotic marker, Annexin V, and the results were similar to the previous measurement. Furthermore, stained cells were then gated into two different populations, Av^+ROS^{low} and Av^+ROS^{high} . As shown in Figure 11, in both HIV-infected and healthy subjects, cells which expressed high apoptotic marker had low levels of ROS, and vice versa. It was also worth noting that the HIV-infected patients expressing higher concentrations of cells had Av^+ROS^{low} , on the other hand, cells that had Av^+ROS^{high} expressed much more in healthy subjects.

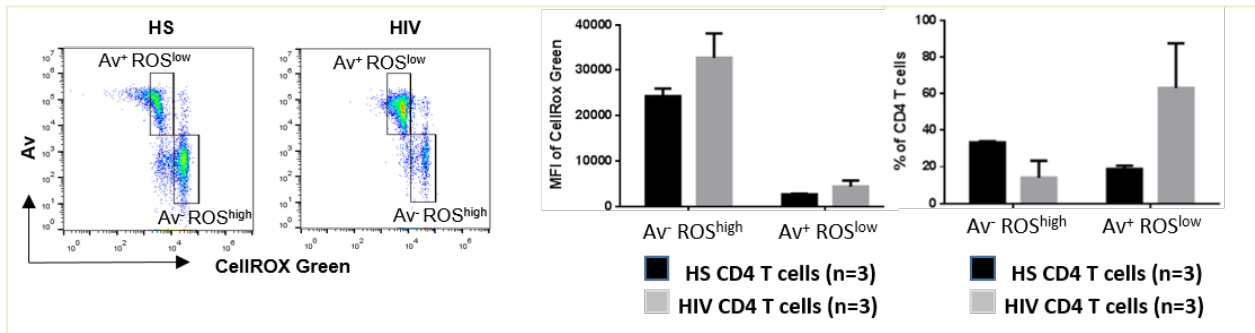


Figure 11: Mean Fluorescence Intensity of CellROX Green and Annexin V in CD4T cells of HIV-infected and healthy subjects. Representative dot plots and summary data of the MFI as well as % of the two gated cell populations ($Av^- ROS^{high}$ and $Av^+ ROS^{low}$) from three subjects in each group are shown. Each dot in the figure represents an individual.

After the determination of telomere length and cellular apoptosis, to further confirm our hypothesis, level of telomeric DNA damages in HIV-infected patients and healthy subjects were measured by immunofluorescence staining and confocal microscope. As mentioned in the Materials and Methods section, the telomeric DNA damage was determined based on the number

of co-localizations of telomeric protein TRF1 and DNA damage marker 53BP1, also called telomere induced foci (TIF).

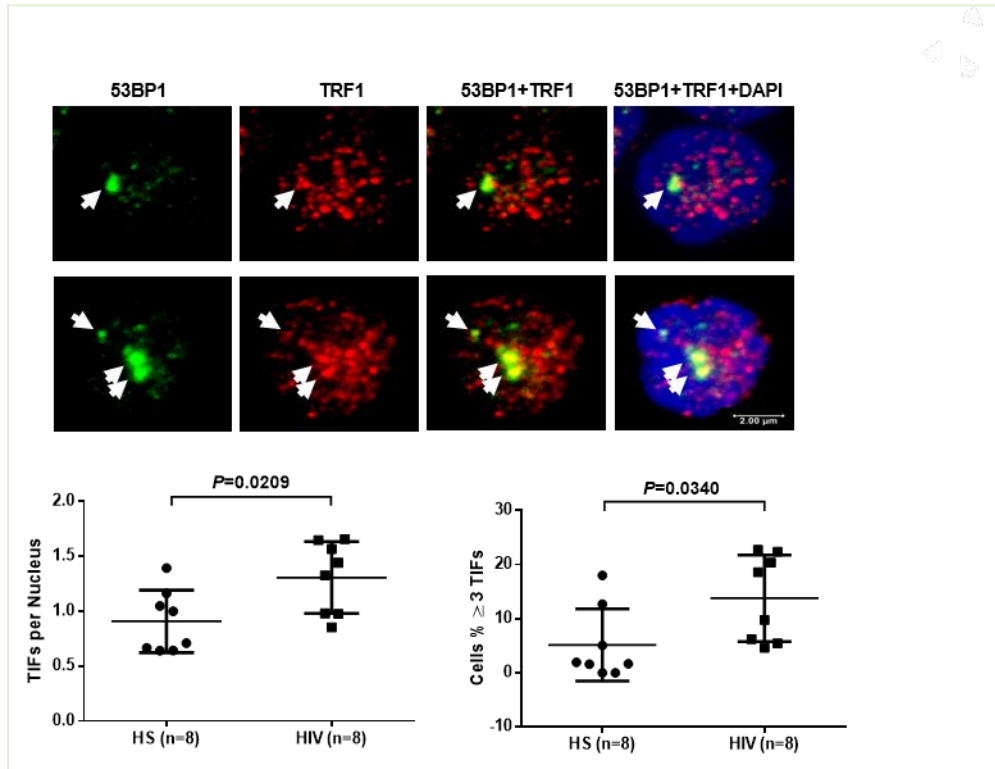


Figure 12: Confocal microscope analysis of the co-localization of 53BP1 and TRF1 proteins

in CD4T cells isolated from HIV-infected and healthy subjects. CD4T cells of 8 subjects from each group were isolated, determined for the co-localization by immunofluorescence assay, and visualized by confocal microscope. The number of telomere induced foci (TIFs) in the nucleus of those cells was also measured. Each dot in the figure represents an individual. The means, \pm SD and p values are also shown.

As shown in Figure 12, the number of TIF per nucleus of cells in HIV-infected patients was significantly higher compared to healthy subjects ($p=0.0029$). In addition, the percentage of

cells which had more than three TIF per cell was also higher in HIV-infected patients (p=0.0340).

Moreover, the expression levels of γ H2AX, a protein considered as a marker of DNA damage, was evaluated in both HIV-infected individuals and healthy subjects by FCM analysis.

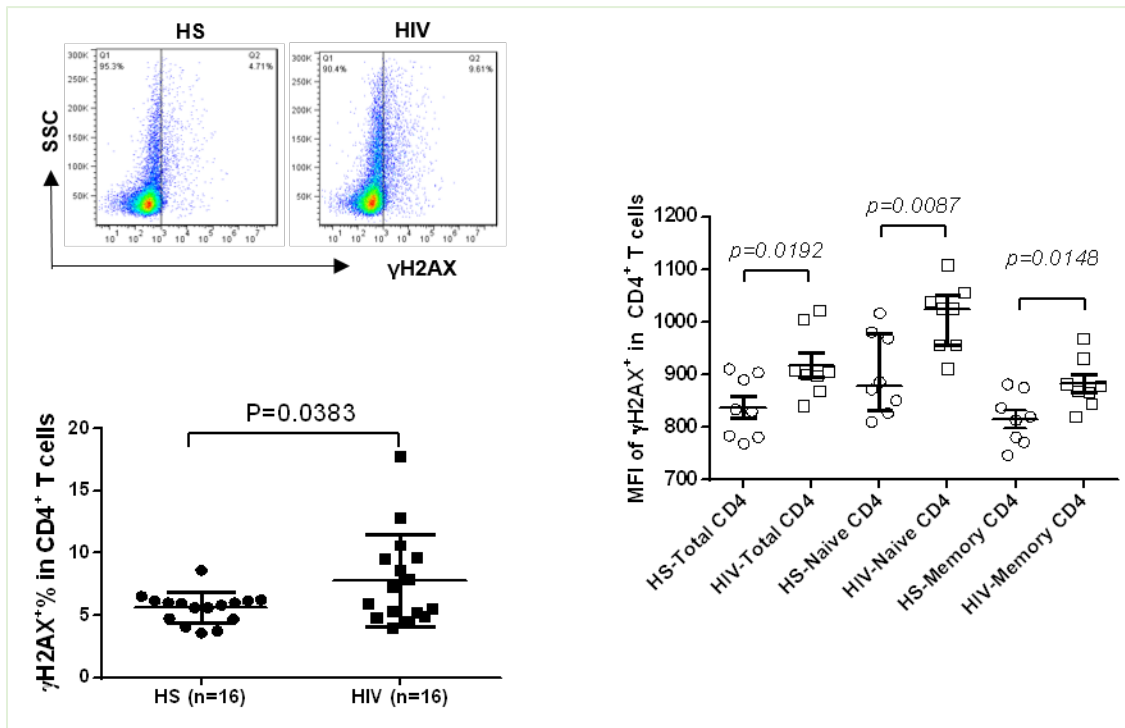


Figure 13: Percentage and Median Fluorescence Intensity of γ H2AX determined by FCM analysis. Total, naïve, and memory CD4T cells of 16 subjects from HIV-infected and healthy subject groups were isolated and determined for γ H2AX percentage and MFI by FCM. Each dot in the figure represents an individual. The means, \pm SD and p values are also shown.

As shown in Figure 13, the MFI level of γ H2AX protein expression of CD4populations in HIV-infected patients was significantly higher compared in healthy subjects, in which the p

value for total CD4 was 0.0192, naïve CD4 was 0.0087 and memory CD4 was 0.0148. Likewise, γ H2AX expression was also higher in HIV-infected subjects with $p=0.0383$. These results suggested that telomere dysfunction caused telomeric DNA damage, which in turn triggered cellular apoptosis in latent HIV infection.

ATM Expression and Activity are Inhibited in CD4 T Cells during Latent HIV Infection

Accumulation of DNA damage and higher incidence of cellular apoptosis indicates that the DDR machineries are not functioning properly as hypothesized. In this project, ATM-related DDR pathway was the main interest. The pathway functions by sending cascade signals from sensors to transducer, further down to mediator and finally is effector proteins. Therefore, any dysfunction of involved proteins could have a great negative impact on the whole system. As mentioned in the Introduction, the sensor of ATM-related DDR is MRN complex, which translocate to the damage site and activates the auto-phosphorylation of transducer protein, ATM kinase. Activated ATM kinase in turn phosphorylates mediators such as CHK2 and p53 proteins, who can further transduce the signal to effector proteins to cause cell cycle arrest and checkpoint activation. In order to investigate the performance of ATM-related DDR pathway, the involved proteins were evaluated by both the transcription level by real-time RT-PCR and translation level by Western Blotting. As shown in Figure 14, the gene and protein expression levels of MRN complex, including MRE11 ($p=0.1830$), RAD50 (0.7124) and NBS1 (0.7920) proteins, were comparable between HIV-infected patients and healthy subjects.

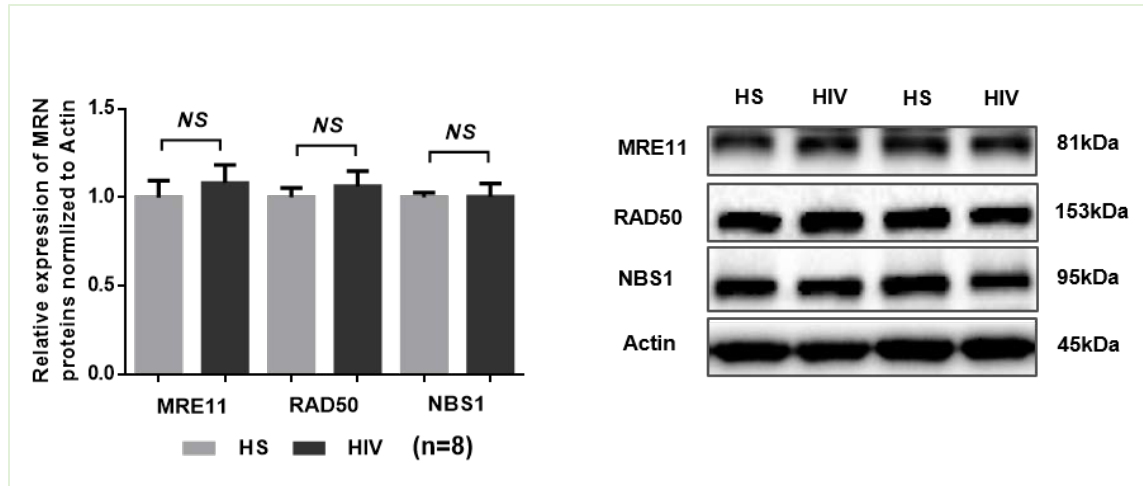


Figure 14: Gene and protein expressions of MRN complex determined by Real-time RT-PCR and Western Blotting, respectively. CD4T cells of 8 subjects from HIV-infected and healthy subject groups were isolated and had their gene and protein expression measured.

Likewise, shown in Figure 15, there was no difference in the gene expression of ATM between the two groups, $p=0.2103$. However, protein expression of both ATM and phosphorylated ATM (p-ATM) proteins, was significantly suppressed in the HIV-infected patients compared to healthy subjects, with $p=0.0107$ and $p=0.0031$, respectively.

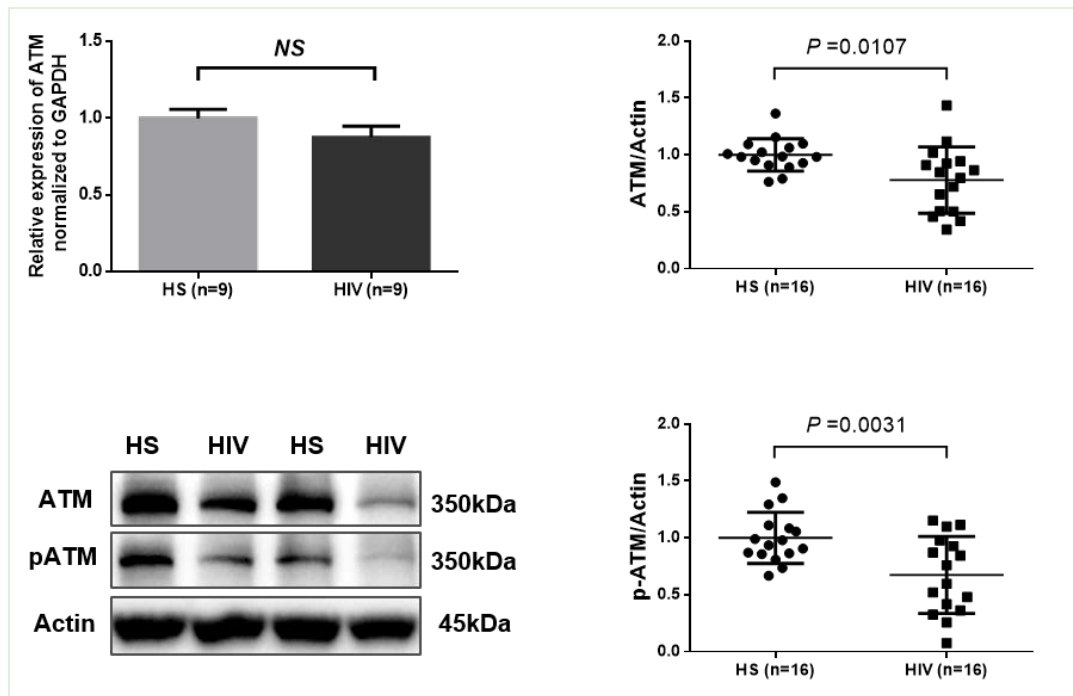


Figure 15: ATM and phosphorylated ATM gene and protein expressions determined by Real-time RT-PCR and Western Blotting. CD4T cells of 9 subjects (for gene expression) and 16 subjects for protein expression from HIV-infected and healthy subject groups were isolated and had their transcription and translation expression levels measured. Each dot in the figure represents an individual. The means, \pm SD and p values are also shown.

To further strengthen the data, ATM protein expressions in CD4populations from HIV-infected individuals and healthy subjected were measured by FCM analysis. As shown is Figure 16, ATM protein expression in all populations of CD4T cells from HIV-infected patients was significantly lower than healthy subjects, in which the p values for total CD4was 0.0060, naïve CD4was 0.0254 and memory CD4was 0.0091. This data confirmed that HIV-infected subjects suffered from ATM deficiency.

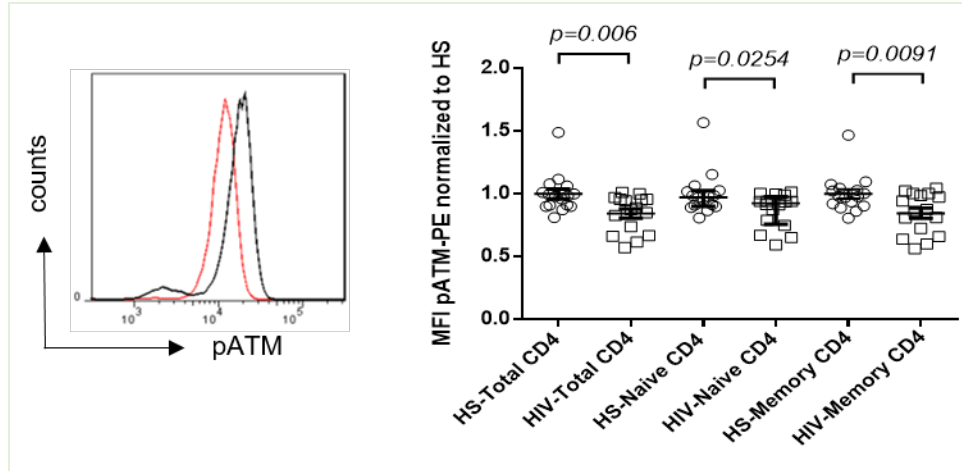


Figure 16: Median Fluorescence Intensity of phosphorylated ATM kinase measured by FCM analysis. Total, naïve, and memory CD4T cells of 8 subjects from HIV-infected and healthy subject groups were isolated and determined for MFI of phosphorylated ATM protein by FCM. Each dot in the figure represents an individual. The means, \pm SD and p values are also shown.

To further investigate the function of ATM-related DDR pathway, the expressions of down-stream proteins involved in the pathway were determined. As shown in Figure 17, while there was no difference in the gene expressions of CHK2 and p53 proteins, the FCM analysis showed that the expression of phosphorylated CHK2 protein was significantly lower in HIV-infected compared healthy subjects.

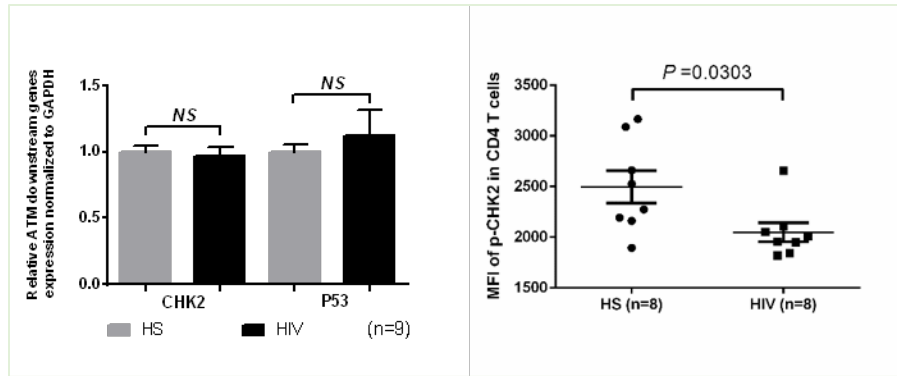


Figure 17: Gene expression and Median Fluorescence Intensity of ATM downstream proteins determined by Real-time RT-PCR. CD4T cells of 9 subjects (for gene expression) and 8 subjects (for MFI detection) from HIV-infected and healthy subject groups were isolated and determined for transcription level and MFI of CHK2 and p53 proteins. Each dot in the figure represents an individual. The means, \pm SD and p values are also shown.

The translation expressions of those proteins were determined by Western Blotting. As shown in Figure 18, there was no difference in p53 protein expression between HIV-infected and healthy subjects, $p=0.6742$. However, the expression of CHK2 was significantly lower in HIV-infected patients, $p=0.0296$. Another thing worth noting is the expression of PARP, a protein involving the DNA repair machinery, and cleaved PARP, which is a cleaved form of PARP after engaging in DNA damage reparation. It can be observed that, the level of PARP expression was significantly lower and cleaved PARP expression was high in HIV-infected subjects, $p=0.0053$. This data suggested that the heart proteins of ATM-related DDR pathway, which were ATM and CHK2, were dysfunctional, causing great affects to the whole crucial pathway, leading to the accumulation of telomeric DNA damage and eventually resulted in cellular apoptosis.

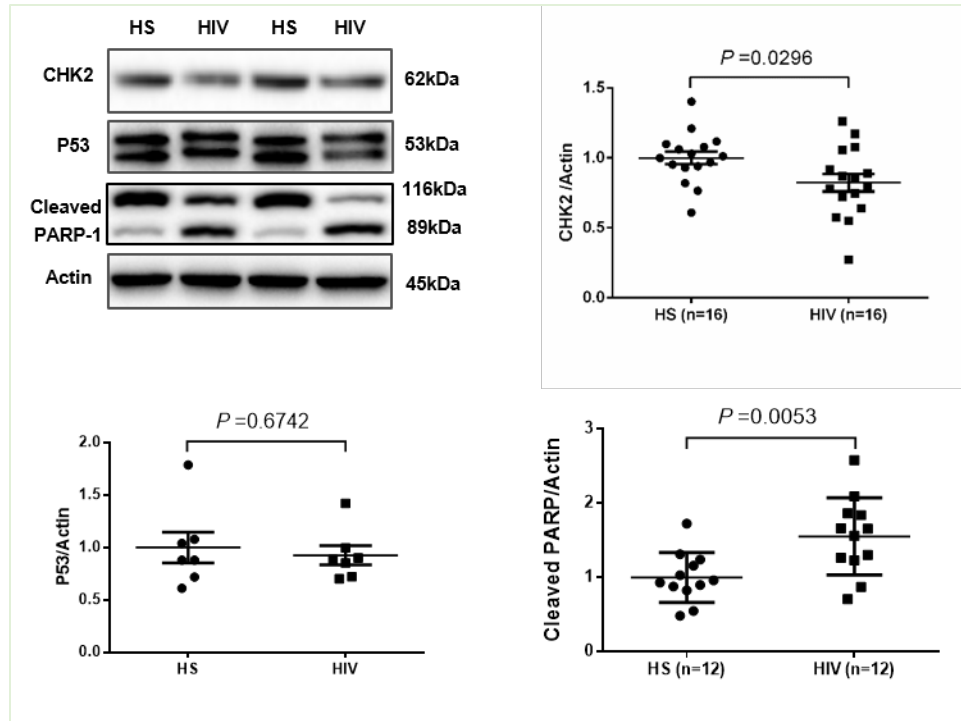


Figure 18: Protein expressions of ATM downstream proteins determined by Western Blotting. CD4T cells of 16 subjects (CHK expression detection) and 12 subjects (cleaved PARP expression detection) from HIV-infected and healthy subject groups were isolated and determined for translation level of CHK2, p53 and cleaved PARP proteins by Western Blotting. Each dot in the figure represents an individual. The means, \pm SD and p values are also shown.

TRF2 Expression and Activity are Inhibited in CD4 T cells during Latent HIV Infection

Until now, all of the collected data had supported the first part of our hypothesis in which the dysfunction of ATM-related DDR pathway resulted in the increase in the accumulation of unrepaired telomeric DNA damages. However, the answer to the question whether it was the only factor that contributed to the DNA damage increase or if other factors were involved, such as the dysfunction of shelterin whose function was to protect the telomere. Our hypothesis was that if any components of this complex did not function properly, it could affect the function of

the whole complex and thus the complex would fail to protect the telomere ends. In order to confirm the hypothesis, the gene and protein expressions of each of the components of the shelterin complex were measured. As shown in Figure 19, there was no significant difference in the gene expression of the shelterin protein between HIV-infected and healthy subjects.

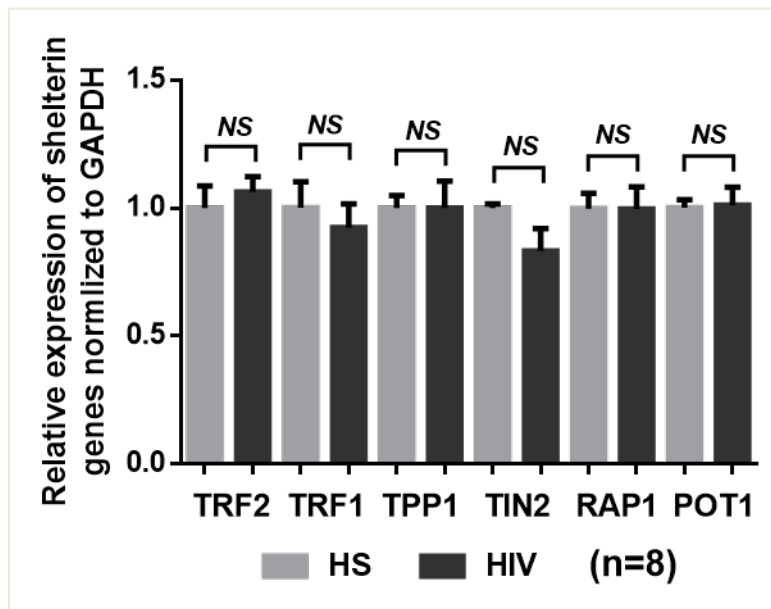


Figure 19: Transcription expressions of proteins in shelterin complex determined by Real-time RT-PCR. CD4T cells of 8 subjects from HIV-infected and healthy subject groups were isolated and determined for transcription levels of shelterin proteins, including TRF1, TRF2, TPP1, TIN2, RAP1 and POT1. The means and \pm SD are also shown.

Furthermore, as shown in Figure 20, there was also no significant difference in the protein expressions of those proteins between the two groups, except for TRF2 protein ($p=0.0163$), whose expression was much lower in HIV-infected patients. This data suggested that

the low expression of TRF2 protein had caused the entire shelterin complex to be compromised, therefore it could not protect the telomere, leading to the increase in the telomeric DNA damage.

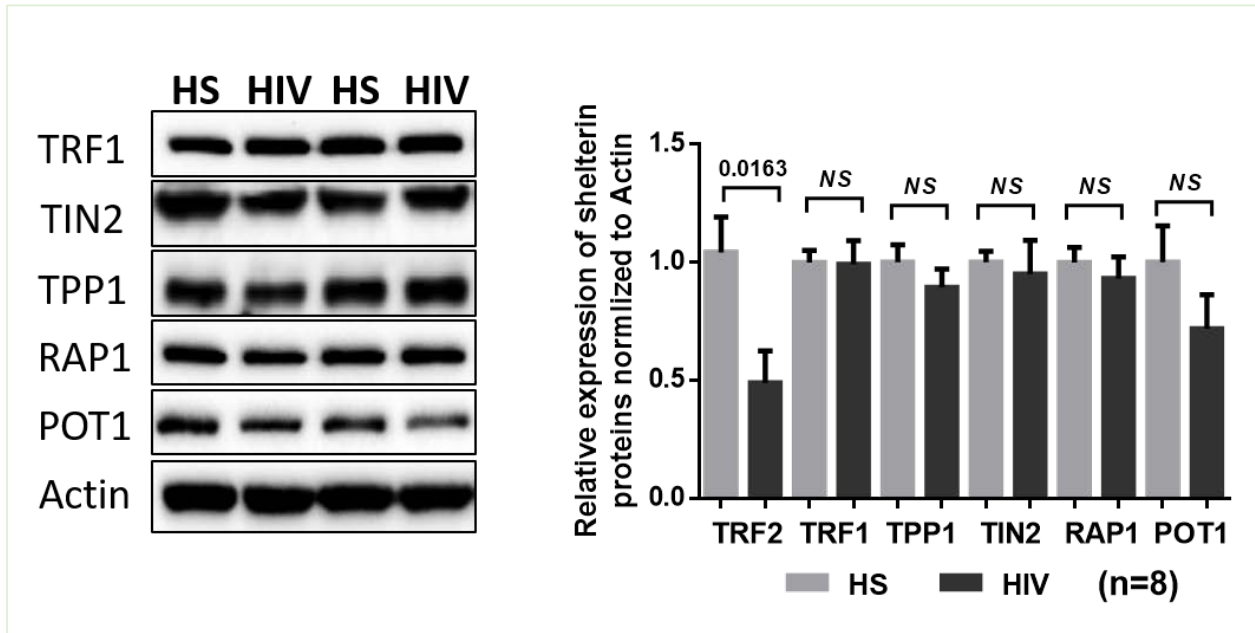


Figure 20: Translation expressions of proteins in shelterin complex determined by Western blotting. CD4T cells of 8 subjects from HIV-infected and healthy subject groups were isolated and determined for translation levels of shelterin proteins, including TRF1, TRF2, TPP1, TIN2, RAP1 and POT1. The means, \pm SD and p values are also shown.

CHAPTER 4

DISCUSSION

T cells play a crucial role in protecting us from pathogens, especially viral infections. The dysfunction of T cells, telomere attrition, as well as failure of the DDR mechanism result in the accumulation of unrepaired DNA damage, cellular senescence, and apoptosis. In this study, we investigated the integrity of the ATM-related DDR pathway and the shelterin complex in latent HIV-infected subjects and compared this to age- matched healthy subjects. We found that the levels of CD4 cells, including its subpopulations such as total, naïve, and memory CD4T cells, were significantly lower in HIV infected subjects than in healthy subjects. Furthermore, these cells were not only suppressed, but also exhibited DNA damage as evidenced by overexpression of DNA damage markers such as γ H2AX, as well as a large number of telomere induced foci in the nucleus when examined under a confocal microscope.

Furthermore, high expression of apoptotic markers, such as PD1 and ROS substances were noted in these dysfunctional CD4T cells. Similarly, the buildup of cellular senescence markers such as CD28 and CD57 were noted in these cells. These markers are an evidence of T cell abnormality and shortened telomere length. This means that the shorter the telomere length, the higher the chances of DNA damage, cellular senescence, and apoptosis.

In addition, we explored a possible mechanism of the cellular dysfunction in these suppressed cells. Our results revealed a flaw in the ATM-related DDR pathway in these HIV-infected individuals. Surprisingly, even though the DNA damage sensor MRN complex remained intact, the expression of ATM kinase (the core of the pathway) was inhibited as evidenced by Western Blotting. Similarly, the expression of CHK2 protein, an important ATM

downstream protein, was noticeably suppressed in these individuals. Due to the inhibition of these key players, the ATM-related DDR pathway failed to repair the persistent DNA damage caused by chronic HIV infection. This caused the accumulation of DNA damaged CD4 cells in the infected individuals.

Following the deficiency of ATM and its downstream CHK2, we tried to ascertain the shelterin integrity. Surprisingly, while there was no abnormality in the gene expressions of TRF1, TIN2, TPP1, POT and RAP1, the expression of TRF2 protein was significantly inhibited in HIV-infected patients compared to healthy subjects. This result suggests that TRF2 could be the key protein protecting the telomeric DNA and as such, its inhibition may be the reason for the poor function of the shelterin complex. These results confirmed our hypothesis as we expected that a bridge in the ATM-related DDR pathway and shelterin integrity could contribute to the DNA damage, cellular senescence, and apoptosis in latent HIV-infected subjects.

The findings in this study have provided fundamental insights for future research in T cell function in latent HIV-infected patients. Since we have established that the expression of ATM and TRF2 proteins are inhibited in HIV infected subjects, this could be further explored. Studies involving knockout of ATM kinase or TRF2 in healthy subjects by siRNA transfection or the use of ATM and TRF2 inhibitors could be done. Similarly, ATM kinase and TRF2 overexpression experiments could be explored in chronic HIV-infected subjects to see if these dysfunctional cells could be rescued from DNA damage and apoptosis. In addition, in vitro studies or the mice models could be used to study the function of these proteins and pathway. Finally, other DDR pathway, such as ATR-related pathway, should also be explored further.

REFERENCES

1. Sharp PM, Hahn BH. 2011. Origins of hiv and the aids pandemic. *Cold Spring Harb Perspect Med.* 1(1):a006841.
2. Klimas N, Koneru AO, Fletcher MA. 2008. Overview of hiv. *Psychosom Med.* 70(5):523-530.
3. Dr Jacqueline Parkin PhD, BryonyCohenBSc. 2001. An overview of the immune system. *The Lancet.* 357:1777-1789.
4. Golubovskaya V, Wu L. 2016. Different subsets of t cells, memory, effector functions, and car-t immunotherapy. *Cancers (Basel).* 8(3).
5. Maartens G, Celum C, Lewin SR. 2014. Hiv infection: Epidemiology, pathogenesis, treatment, and prevention. *The Lancet.* 384(9939):258-271.
6. Naif HM. 2013. Pathogenesis of hiv infection. *Infect Dis Rep.* 5(Suppl 1):e6.
7. Okoye AA, Picker LJ. 2013. Cd4(+) t-cell depletion in hiv infection: Mechanisms of immunological failure. *Immunol Rev.* 254(1):54-64.
8. Planelles V. 2017. When DNA damage is acceptable. *Cell Cycle.* 16(11):1020-1021.
9. Perfettini JL, Nardacci R, Bourouba M, Subra F, Gros L, Seror C, Manic G, Rosselli F, Amendola A, Masdehors P et al. 2008. Critical involvement of the atm-dependent DNA damage response in the apoptotic demise of hiv-1-elicited syncytia. *PLoS One.* 3(6):e2458.
10. Piekna-Przybylska D, Sharma G, Maggirwar SB, Bambara RA. 2017. Deficiency in DNA damage response, a new characteristic of cells infected with latent hiv-1. *Cell Cycle.* 16(10):968-978.
11. Blackford AN, Jackson SP. 2017. Atm, atr, and DNA-pk: The trinity at the heart of the DNA damage response. *Mol Cell.* 66(6):801-817.

12. Marechal A, Zou L. 2013. DNA damage sensing by the atm and atr kinases. *Cold Spring Harb Perspect Biol.* 5(9).
13. Lavin MF, Kozlov S. 2007. Atm activation and DNA damage response. *Cell Cycle.* 6(8):931-942.
14. Tamar Uziel, Yaniv Larenthal, Lilach Moyal, Yair Andegeko, Leonid Mittelman and Yosef Shiloh. 2003. Requirement of the MRN complex for ATM activation by DNA damage. *The EMBO Journal.* 22(20):5612-5621.
15. Burma S, Chen BP, Murphy M, Kurimasa A, Chen DJ. 2001. Atm phosphorylates histone h2ax in response to DNA double-strand breaks. *J Biol Chem.* 276(45):42462-42467.
16. Perkhofer L, Schmitt A, Romero Carrasco MC, Ihle M, Hampp S, Ruess DA, Hessmann E, Russell R, Lechel A, Azoitei N et al. 2017. Atm deficiency generating genomic instability sensitizes pancreatic ductal adenocarcinoma cells to therapy-induced DNA damage. *Cancer Res.* 77(20):5576-5590.
17. Petr Starostik, Taghi Manshouri, Susan O'Brien, Kniil Freireich, Hagop Kantarjian, Mohammad Haidar, Susan Lerner, Michael Keating, and Maher Albitar. 1998. Deficiency of the ATM Protein Expression Defines an Aggressive Subgroup of B-Cell Chronic Lymphocytic Leukemia. *CANCER RESEARCH.* 58:4552-4557.
18. Shao L, Fujii H, Colmegna I, Oishi H, Goronzy JJ, Weyand CM. 2009. Deficiency of the DNA repair enzyme atm in rheumatoid arthritis. *J Exp Med.* 206(6):1435-1449.
19. Kim JJ, Lee SB, Yi SY, Han SA, Kim SH, Lee JM, Tong SY, Yin P, Gao B, Zhang J et al. 2017. Wsb1 overcomes oncogene-induced senescence by targeting atm for degradation. *Cell Res.* 27(2):274-293.

20. Winkler J, Hofmann K, Chen S. 2014. Novel targets for atm-deficient malignancies. *Mol Cell Oncol.* 1(1):e29905.
21. J Boulton. 2001. Ataxia telangiectasia gene mutations in leukemia and lymphoma. *J Clin Pathol.* 54:512–516.
22. Blackburn EH. 1991. Structure and function of telomeres. *Nature.* 350(6319):569-573.
23. Zakian VA. 1989. Structure and function of telomeres. *Annual Review of Genetics.* 23(1):579-604.
24. Erdel F, Kratz K, Willcox S, Griffith JD, Greene EC, de Lange T. 2017. Telomere recognition and assembly mechanism of mammalian shelterin. *Cell Rep.* 18(1):41-53.
25. Kim H, Li F, He Q, Deng T, Xu J, Jin F, Coarfa C, Putluri N, Liu D, Songyang Z. 2017. Systematic analysis of human telomeric dysfunction using inducible telosome/shelterin crispr/cas9 knockout cells. *Cell Discov.* 3:17034.
26. Fumagalli M, Rossiello F, Clerici M, Barozzi S, Cittaro D, Kaplunov JM, Bucci G, Dobrev M, Matti V, Beausejour CM et al. 2012. Telomeric DNA damage is irreparable and causes persistent DNA-damage-response activation. *Nat Cell Biol.* 14(4):355-365.
27. Sun L, Tan R, Xu J, LaFace J, Gao Y, Xiao Y, Attar M, Neumann C, Li GM, Su B et al. 2015. Targeted DNA damage at individual telomeres disrupts their integrity and triggers cell death. *Nucleic Acids Res.* 43(13):6334-6347.
28. Shtessel L, Ahmed S. 2011. Telomere dysfunction in human bone marrow failure syndromes. *Nucleus.* 2(1):24-29.
29. Laure Crabbe, Anna Jauch, Colleen M. Naeger, Heidi Holtgreve-Grez, and Jan Karlseder. 2007. Telomere dysfunction as a cause of genomic instability in Werner syndrome. *PNAS.* 104(70): 2205–2210.

30. Zhao J, Dang X, Zhang P, Nguyen LN, Cao D, Wang L, Wu X, Morrison ZD, Zhang Y, Jia Z et al. 2018. Insufficiency of DNA repair enzyme atm promotes naive cd4 t-cell loss in chronic hepatitis c virus infection. *Cell Discov.* 4:16.
31. Nguyen LN, Zhao J, Cao D, Dang X, Wang L, Lian J, Zhang Y, Jia Z, Wu XY, Morrison Z et al. 2018. Inhibition of trf2 accelerates telomere attrition and DNA damage in naive cd4 t cells during hcv infection. *Cell Death Dis.* 9(9):900.
32. Kleiveland CR. 2015. Peripheral blood mononuclear cells. In: Verhoeckx K, Cotter P, Lopez-Exposito I, Kleiveland C, Lea T, Mackie A, Requena T, Swiatecka D, Wichers H, editors. *The impact of food bioactives on health: In vitro and ex vivo models.* Cham (CH). p. 161-167.
33. Michael Brown and Carl Wittwer. 2000. *Flow Cytometry: Principles and Clinical Applications in Hematology.* *Clinical Chemistry.* 46:8(B) 1221–1229.
34. Elmore S. 2007. Apoptosis: A review of programmed cell death. *Toxicol Pathol.* 35(4):495-516.
35. Redza-Dutordoir M, Averill-Bates DA. 2016. Activation of apoptosis signalling pathways by reactive oxygen species. *Biochim Biophys Acta.* 1863(12):2977-2992.
36. Wlodkowic D, Telford W, Skommer J, Darzynkiewicz Z. 2011. Apoptosis and beyond: Cytometry in studies of programmed cell death. *Methods Cell Biol.* 103:55-98.
37. Guohong Zhang, Vanessa Gurtu, Steven R. Kain and Guochen Yan. 1997. Early Detection of Apoptosis Using a Fluorescent Conjugate of Annexin V. *BioTechniques.* 23:525-531.
38. Abu-Qare AW, Abou-Donia MB. 2001. Biomarkers of apoptosis: Release of cytochrome c, activation of caspase-3, induction of 8-hydroxy-2'-deoxyguanosine, increased 3-

- nitrotyrosine, and alteration of p53 gene. *Journal of Toxicology and Environmental Health Part B: Critical Reviews*. 4(3):313-332.
39. H.-U. Simon, A. Haj-Yehia and F. Levi-Schaffer. 2000. Role of reactive oxygen species (ROS) in apoptosis induction. *Apoptosis*. 5: 415–418.
40. Gutierrez-Rodrigues F, Santana-Lemos BA, Scheucher PS, Alves-Paiva RM, Calado RT. 2014. Direct comparison of flow-fish and qpcr as diagnostic tests for telomere length measurement in humans. *PLoS One*. 9(11):e113747.

VITA

LAM NGOC THAO NGUYEN

Education: Master of Science in Biology, East Tennessee State University,

Biological Sciences Department, 2019

Bachelor in Biotechnology, Ho Chi Minh International University,

Ho Chi Minh City, Viet Nam, 2016

Professional Experience: Graduate Assistant, East Tennessee State University,

Biological Sciences Department, 2019